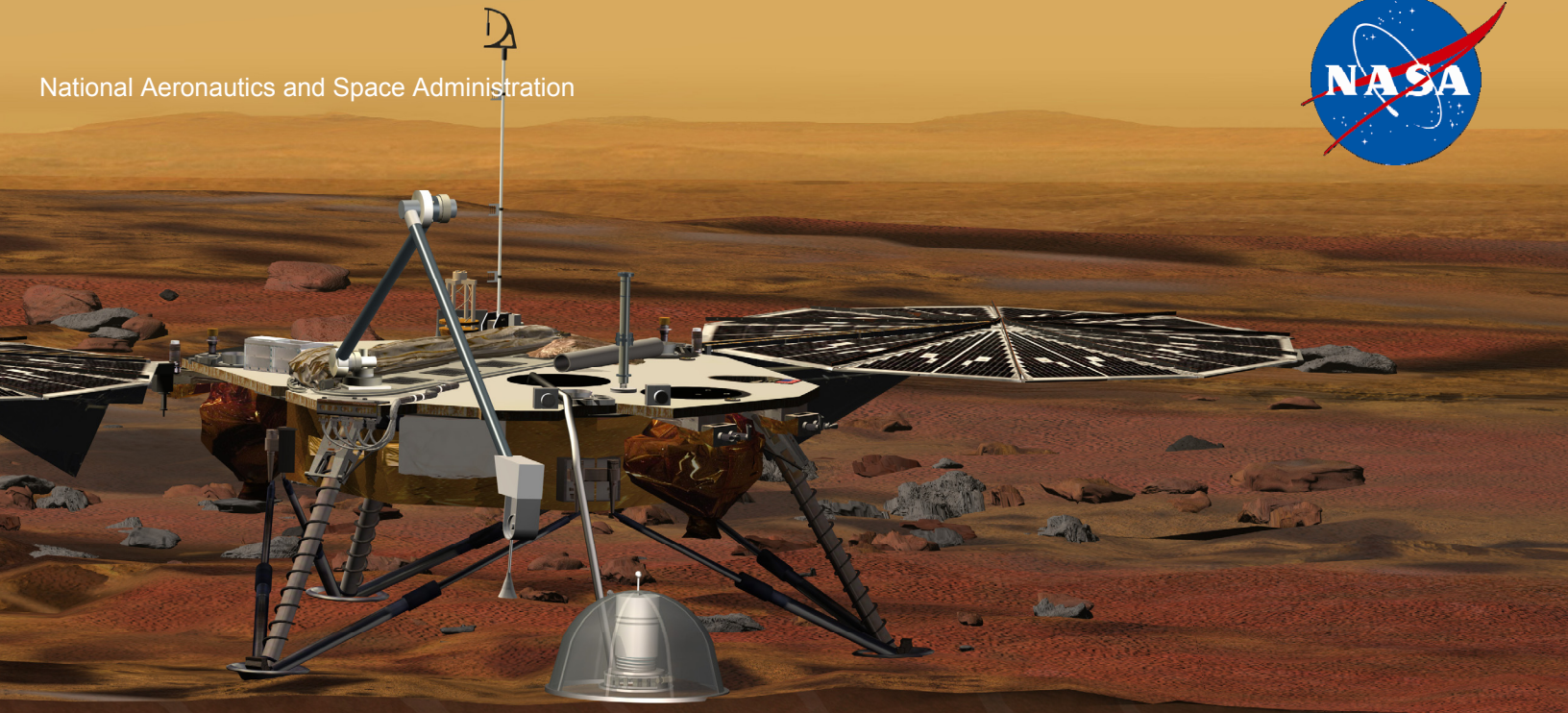


National Aeronautics and Space Administration



Mission Concept Study

Planetary Science Decadal Survey Mars Geophysical Network

Science Champion: Dr. Lindy Elkins-Tanton (ltelkins@mit.edu)

NASA HQ POC: Lisa May (lisa.may@nasa.gov)

June 2010

Data Release, Distribution, and Cost Interpretation Statements

This document is intended to support the SS2012 Planetary Science Decadal Survey.

The data contained in this document may not be modified in any way.

Cost estimates described or summarized in this document were generated as part of a preliminary concept study, are model-based, assume a JPL in-house build, and do not constitute a commitment on the part of JPL or Caltech. References to work months, work years, or FTEs generally combine multiple staff grades and experience levels.

Cost reserves for development and operations were included as prescribed by the NASA ground rules for the Planetary Science Decadal Survey. Unadjusted estimate totals and cost reserve allocations would be revised as needed in future more-detailed studies as appropriate for the specific cost-risks for a given mission concept.

Planetary Science Decadal Survey

Mission Concept Study Final Report

Study Participants	v
Acknowledgments	vi
Executive Summary	vii
1. Scientific Objectives	1
Science Questions and Objectives	1
Science Traceability	6
2. High-Level Mission Concept	7
Overview	7
Concept Maturity Level	7
Technology Maturity.....	8
Key Trades.....	8
Cruise Stage Architecture	10
3. Technical Overview	11
Instrument Payload Description	11
Potential Additional Instruments	18
Flight System	23
Concept of Operations and Mission Design.....	30
Planetary Protection.....	35
Risk List	36
4. Development Schedule and Schedule Constraints	39
High-Level Mission Schedule.....	39
Technology Development Plan	40
Development Schedule and Constraints.....	40
ATLO Flow for Two Landers	40
5. Mission Life-Cycle Cost	41
Costing Methodology and Basis of Estimate	41
Cost Estimates.....	41

Figures

Figure 2-1. Typical Orientation for Mars Surface Spacecraft.....	9
Figure 2-2. Concept of a Two-Lander Stacked Configuration	9
Figure 2-3. Concept of a Two-Lander Vertical Configuration	9
Figure 3-1. SEIS showing the evacuated sphere where the VBB sensors are located, the base, and support structure.....	13
Figure 3-2. Response and noise curves for the seismometer.	13
Figure 3-3. IDA end effector and ball-on-stalk device for picking up and placing SEIS on the ground.	14
Figure 3-4. Navcam Camera on Which the IDC Would be Based.....	14
Figure 3-5. Hot-wire Anemometer Details and Operational Principle.....	17
Figure 3-6. Sonic anemometer (left) and a photograph of the electro-static transducers that enable sonic anemometry at Mars (right)	21
Figure 3-7. EDL Sequence (Legged Lander).....	32
Figure 3-8. Mars Landing Sites.....	33
Figure 3-9. Risk Chart	36
Figure 4-1. Mission Schedule.....	39

Tables

Table 1-1. Science Traceability Matrix.....	6
Table 2-1. Concept Maturity Level Definitions	8
Table 3-1. Payload Mass and Power	11
Table 3-2. SEIS	13
Table 3-3. Instrument Deployment Camera.....	15
Table 3-4. Stereocams (Two).....	15
Table 3-5. ATM (P, T, W).....	18
Table 3-6. HP ³	19
Table 3-7. Electromagnetic Sounder	20
Table 3-8. Atmospheric Dust Sensors (Two).....	22
Table 3-9. Flight Element Masses	23
Table 3-10. Lander Mass and Power.....	25
Table 3-11. Lander Characteristics.....	25
Table 3-12. Entry System Mass and Power.....	27
Table 3-13. Entry System Characteristics.....	27
Table 3-14. Cruise Stage Mass and Power	29
Table 3-15. Cruise Stage Characteristics	29
Table 3-16. Earth-Mars 2022 Type I Trajectory with Launch Window.....	31

Table 3-17. Mission Design.....	33
Table 3-18. Mission Operations and Ground Data Systems	34
Table 3-19. DSN Tracking Schedule	35
Table 3-20. Detailed Risk Description and Mitigation Strategy.....	37
Table 3-21. Risk Level Definitions	38
Table 4-1. Key Phase Duration.....	40
Table 5-1. Science Costs by Phase (FY 2015).....	42
Table 5-2. Science Workforce by Phase.....	42
Table 5-3. Total Mission Cost Funding Profile	43

Appendices

- A. Acronyms
- B. References

Study Participants

Role	Participant	Affiliation
Study Lead	Eric Klein	Jet Propulsion Laboratory
Mars Panel Advocate Team		
Science Champion	Dr. Lindy Elkins-Tanton	Massachusetts Institute of Technology
Science	Philippe Lognonné	Institut de Physique du Globe de Paris
Technical /Management	Glenn Cunningham	Consultant
Science	Wendy Calvin	University of Nevada, Reno
JPL Study Team		
Science	Bruce Banerdt	Jet Propulsion Laboratory
Systems Engineer	Joan Ervin	Jet Propulsion Laboratory
Systems Engineer / Programmatic	Cate Heneghan	Jet Propulsion Laboratory
Instruments	Kenneth Hurst	Jet Propulsion Laboratory
Mission Design / EDL	Evgeniy Sklyanskiy	Jet Propulsion Laboratory
Systems Engineer	Greg Wilson	Jet Propulsion Laboratory
Advanced Project Design Team (Team X)		
Mechanical	Christopher Landry	Jet Propulsion Laboratory
Ground Systems	Greg Welz	Jet Propulsion Laboratory
Planetary Protection	Laura Newlin	Jet Propulsion Laboratory
Programmatic / Risk	Jairus Hihn	Jet Propulsion Laboratory
Propulsion	Frank Picha	Jet Propulsion Laboratory
Science	William Smythe	Jet Propulsion Laboratory
Mission Design	Try Lam	Jet Propulsion Laboratory
JPL SS 2012 PSDS Lead	Kim Reh	Jet Propulsion Laboratory
NASA HQ POC	Lisa May	National Aeronautics and Space Administration

Acknowledgments

This research was carried out at the Jet Propulsion Laboratory, California Institute of Technology, under a contract with the National Aeronautics and Space Administration.

© 2010. All rights reserved.

Executive Summary

The science objectives of the Mars Geophysical Network (MGN) mission study were divided into two categories: primary (the science floor that would need to be addressed to justify the mission) and secondary (additional goals that prospective principal investigators would reasonably add, given sufficient resources). By request from the Planetary Science Decadal Survey Mars Panel, this study addressed only the primary objective—to characterize the internal structure of Mars to better understand its early history and internal processes affecting its surface and habitability. Measurement requirements included characterization of crustal structure and thickness, investigation of mantle compositional structure and phase transitions, and characterization of core size, density, state, and structure.

The purpose of the study was to determine if MGN could accomplish this science objective within the resource constraints of NASA's New Frontiers Program.

An initial trade study was conducted on several mission configurations for MGN to evaluate science return, cost, and mission risk [1]. Strategies for launch, interplanetary cruise, and targeting for entry, descent, and landing (EDL) on the surface of Mars vary as the number of landed network nodes increases from one to three. The Mars Panel selected a two-lander mission concept for further study. The selected EDL architecture for this study uses a powered descent lander. This is a low-to-medium risk concept. The most significant mission risks are related to navigation errors, entry, descent and landing (EDL) failure, and communication link failure. The powered lander concept in this design is an evolution from successful concepts used in the recent past such as the Phoenix lander. No new technologies are required. Two identical free-flying vehicles would be launched on a single Atlas V 401 independently targeted for Mars entry seven days apart and land at geographically distributed sites appropriate to meet science operational objectives.

For the MGN concept, surface operations would be for one Mars year or approximately two Earth years. The main instrument would be a pair of seismometers that would monitor surface movement. Each seismometer would be located on a separate lander. The seismic measurements would be complemented by precision tracking of the landers through direct-to-Earth Doppler tracking using the spacecraft's X-band communication system (requiring no additional hardware). The landers would be several thousand kilometers apart. Other instruments that would be carried in support of each seismometer include a robotic arm (with supporting engineering cameras) and an atmospheric instrument suite. The arm would place the seismometer on the surface at the start of science operations. After that, the arm would not be used. Cameras would be located on the arm and fixed on the deck to aid with deployment of the seismometer from the deck to the ground. The atmospheric instrument suite would be used to help understand the noise in the seismometer data, some of which originates from interaction of the atmospheric temperature, pressure, and wind with the ground or the instrument. An improved 3D high frequency anemometer would permit new investigations with respect to interactions between the surface and the atmospheric boundary layer. Two additional instruments, an electromagnetic sounder and heat flow probe, could also be included to further expand the science value of the mission. These are described below, but are not included in the point design described in this report.

Though a dedicated Advanced Project Design Team (Team X) study was not conducted for MGN, the mission concept presented here draws heavily from the results of previous Jet Propulsion Laboratory (JPL) missions and recent Team X studies. Results of this study as described in the report indicate that this mission would likely be achievable within the New Frontiers mission cost cap.

1. Scientific Objectives

Science Questions and Objectives

Science Questions

The Mars Geophysical Network (MGN) would be a two-lander mission with geophysical instrumentation to study the interior of Mars. Investigations enabled by simultaneous geophysical observations at multiple points on the surface would allow, for the first time, detailed characterization of the interior of a terrestrial planet other than Earth. This would yield invaluable information about the early processes that formed the planets and subsequently shaped their surfaces and provide crucial insight into the evolution of habitability on Mars.

Our fundamental understanding of the interior of Earth comes from geophysics, geochemistry, and petrology. For geophysics, surface heat flow, magnetic, paleomagnetic, and gravity field measurements, electromagnetic (EM) techniques and, particularly, seismology have revealed the basic internal layering of Earth, its thermal structure and its gross compositional stratification, and significant lateral variations in these quantities. Understanding how life developed and evolved on Earth requires knowledge of Earth's thermal and volatile evolution and how mantle and crustal heat transfer and volatile release affected habitability at and near the planet's surface.

Mars' evolution is in sharp contrast to that of Earth's. Earth's thermal engine has transferred heat to the surface largely by lithospheric recycling (plate tectonics) over much of its history; there is little evidence that this process ever occurred on Mars. The signature of early planetary processes may be preserved in Mars' internal structure, making it a particularly desirable candidate for geophysical investigation. Although Earth has lost the structures caused by differentiation and early evolution because of vigorous mantle convection, Mars may retain evidence, such as azimuthal and radial compositional differentiation in the mantle. Furthermore, much of the martian crust dates back to the first half billion years of the solar system [2]. Measurements of the planetary interior may therefore detect structures created during differentiation and early evolution, making Mars an ideal subject for understanding planetary accretion and early evolution.

Planetary interiors not only record evidence of conditions of planetary accretion and differentiation, they exert significant control on surface environments. The structure of a planet's interior and its dynamics control heat transfer within a planet through advected mantle material, heat conducted through the lithosphere, and volcanism. Volcanism in particular controls the timing of volatile release and influences the availability of water and carbon. The existence and strength of any planetary magnetic field depends in part on the size and state of the core.

The crust of a planet is generally thought to form initially through fractionation of an early magma ocean, with later addition through partial melting of the mantle and resulting volcanism. Thus, the volume (thickness) and structure of the crust can place constraints on the evolution of the putative martian magma ocean and, by extension, planetary magma oceans in general. Currently, the volume of Mars' crust is unknown to within a factor of two.

Knowledge of the state of Mars' core and its size is important for understanding the planet's evolution. The thermal evolution of a terrestrial planet can be deduced from the dynamics of its mantle and core. The state of the core depends on the percentage of light elements in the core and on the core temperature, which is related to the heat transport in the mantle [3-6]. Thus, the present size and state of the core have important implications for understanding the evolution and present state of Mars [3, 7-11].

Mantle dynamics is essential in shaping the geology of the surface through volcanism and tectonics [11]. The radius of the core has implications for possible mantle convection scenarios and in particular for the presence of a perovskite phase transition at the bottom of the mantle, which enables global plume-like features to exist and persist over time [12].

A geophysical reconnaissance of Mars should reveal at a minimum the basic radial compositional structure: the crust, the upper and lower mantle, and the solid and/or liquid core. Considerable value would also derive from placing strong constraints on the radial thermal structure. The compositional structure relates to the bulk composition of the planet and early differentiation and fractionation of the interior. Thermal structure is derived from the radial seismic velocity structure (particularly, phase boundaries), supplemented by heat flow measurements and EM sounding, and provides the “end condition” on thermal evolution scenarios. To gain full appreciation of heat transfer processes, lateral variations in mantle thermal structure must be derived from a geophysical network with an adequate distribution of stations. Strong thermal anomalies very likely remain in the mantle and the lithosphere very likely varies in thickness from hot spot processes; in fact, without this lateral information, the average radial geophysical properties may not be well determined.

The four primary methods for geophysically probing a planet’s interior from its surface are seismology, precision tracking (for rotation measurements), heat flow, and EM sounding. Each of these methods is discussed in more detail below.

Prioritized Science Objectives

The prioritized science objectives for MGN that address the questions described above are as follows:

1. Characterize the internal structure of Mars to better understand its early planetary history and internal processes affecting its surface and habitability.
 - a. Characterize crustal structure and thickness.
 - b. Investigate mantle compositional structure and phase transitions.
 - c. Characterize core size, density, state and structure.
2. Characterize the thermal state of Mars to better understand its early planetary history and internal processes affecting the surface and habitability.
 - a. Measure crustal heat flow.
 - b. Characterize thermal profile with depth.
3. Characterize the local meteorology and provide ground truth for orbital climate measurements.
 - a. Measure the properties related to atmospheric thermodynamics and motion

Objective 1 is considered the minimum science floor to justify MGN, with objectives 2 and 3 considered secondary.

Measurements

The best understanding of the interior of Mars would come from the synergistic analysis of many different geophysical data sets. Seismology, precision tracking, heat flow, and EM sounding have been identified by several working groups as the key measurement techniques. Seismology is acknowledged to be by far the most valuable and effective of the methods to understand the interior of Mars. Even in the absence of complementary information on thermal state and resistivity, major advances in knowledge would be achieved by seismic measurements alone. In addition to the interior science objectives, it is recognized that meteorological measurements are particularly well served by simultaneous measurements at multiple locations on the surface. Thus, characterization of local weather processes is included as a secondary objective.

Therefore, seismology and precision tracking, which does not require additional hardware beyond the spacecraft telecommunication system, are considered the baseline payload for the MGN mission concept. Though EM sounding, heat flow, and more sophisticated atmospheric instruments are not included in this point design, the capabilities and requirements of each of these investigations are described below.

Seismology

The degree of martian seismic activity remains unknown because of the high sensitivity to wind and poor installation of the Viking seismometer [13,14]. However, from models of the thermoelastic cooling of the lithosphere and extrapolation from visible faults [15-17], seismic activity approximately 100 times higher than that on the Moon has been estimated. Such a model [16] predicts approximately 100 quakes per year with seismic moment greater than 10^{14} Nm (magnitude $M_w = 3.3$) and one per year of seismic moment greater than 10^{17} Nm ($M_w = 5.3$). Impacts provide additional seismic sources and are estimated to occur at a rate similar to that of the Moon [18]. Together with estimates of seismic properties of Mars, which have been studied extensively in the last two decades [19-23], strong and conservative constraints can be used for estimating the amplitude of seismic waves. This leads to well-defined sensitivity requirements for seismic instrumentation needed to characterize the signals from a sufficient number of events and produce enough seismic data for useful analysis (see Table 1-1).

In order to fully reach the science goals described above, seismic investigations would require a network of at least four stations: three with a spacing of approximately 3,000 km (i.e., 50°) and an antipodal station capable of detecting seismic waves traveling through the core from an event simultaneously detected by the others. Such a network might locate, through travel-time analysis, more than 80 quakes per (Earth) year and would be robust to unexpected high mantle attenuation or low seismic activity. With four or more landers, fine details of the internal structure, such as the dichotomy or other large unit differences, mantle discontinuities, and anisotropy, might also be characterized.

A two-station network is considered the minimum network size to address the baseline science of MGN. Determination of the internal structure is also possible with fewer stations under certain assumptions, if they are provided with the highest quality instruments. With data from two seismic stations, true seismic events should be readily distinguishable from local noise, and approximate locations of events could be determined using reasonable assumptions. If both are located near a seismically active region (e.g., Tharsis), they should be able to detect sufficient shallow quakes, in addition to meteorite impacts, to model the upper mantle beneath the two landers. Two stations allow the velocity dispersion analysis of surface waves from larger quakes. Atmospherically generated seismic “noise” could also provide mean phase velocities of surface waves (and thus crustal and upper mantle structure) using the cross-correlation techniques [24]. In addition, the data from each station could be analyzed using advanced single-station seismic techniques, such as receiver function analysis, solid tide measurements, and possibly normal modes.

Precision Tracking—Geodesy

Precision tracking of the martian surface would be performed through radio links between ground stations on Earth and landers on the surface of Mars. The experiment would consist of an X-band (or Ka-band) transponder designed to obtain two-way Doppler and/or ranging measurements from the radiometric link. These Doppler measurements, taken over a long period of time (at least one martian year), could be used to obtain Mars’ rotation behavior (i.e., precession, nutations, and length-of-day variations). The ultimate objectives of this experiment are to obtain information on Mars’ interior and on the mass redistribution of CO_2 in Mars’ atmosphere. Precession (long-term secular changes in the rotational orientation) and nutations (periodic changes in the rotational orientation) as well as polar motion (motion of the planet with respect to its rotation axis) would be determined from this experiment and used to obtain information about Mars’ interior. At the same time, measurement of variations in Mars’ rotation rate could determine variations of the angular momentum due to seasonal mass transfer between the atmosphere and ice caps [24-36].

Precession determination would improve the determination of the moment of inertia of the whole planet and the radius of the core. For a specific interior composition or even for a range of possible compositions, the core radius is expected to be determined with a precision of a few tens of kilometers. A precise measurement of variations in the orientation of Mars’ spin axis would also enable, in addition to the determination of the moment of inertia of the core, an even better determination of the size of the core via the core resonance in the nutation amplitudes. A large inner core can also have an effect on the nutations that could be measured by radio tracking due to the existence of resonance in the free inner core nutation.

A great deal has already been learned from such experiments on Viking and Mars Pathfinder (MPF), but better accuracy than Viking (≤ 0.1 mm/s) and a longer time span than MPF (which lasted ~ 60 sols) are necessary for significant advances.

Enhancement Options: Heat Flow, Electromagnetic Sounding, and Boundary Layer Meteorology

Heat Flow: Planetary heat flow is a fundamental parameter characterizing the thermal state of a planet. Knowledge of the present-day heat flux on Mars would elucidate the workings of the planetary heat engine and provide essential boundary conditions for models of the martian thermal evolution. This would enable us to discriminate between different evolution models, all of which have different predictions for when the dynamo was active. A determination of the average heat flow would also provide important constraints on the abundance of radioactive isotopes in the martian interior, which in turn would place limits on the major element chemistry. By measuring the mantle contribution to the heat flow in regions of thin crust (e.g., the Hellas basin), questions concerning the distribution of heat-producing elements between crust and mantle and the process of planetary differentiation could also be addressed.

Planetary heat flow determines the depth at which liquid water is stable below the surface and thus directly bears on this critical habitability parameter [37]. Furthermore, geothermal energy (i.e., heat flow) is the most important energy source in the martian subsurface today and knowledge of the planetary heat flow would directly constrain the potential for biological activity on present-day Mars.

To measure heat flow, the thermal conductivity and thermal gradient in the regolith need to be determined. This would be achieved by emplacing temperature sensors and heaters in the subsurface. Thermal conductivity would then be determined by active heating experiments or an analysis of the decay of the annual temperature wave. Measurement uncertainties for the thermal conductivity and thermal gradient measurements should be below 10% each, resulting in an uncertainty of 15% for the heat flow. To achieve this accuracy, temperature sensors would need to be calibrated to within 0.1 degree K.

The heat flow from the interior is expected to be similar in large provinces on the martian surface. The measurement sites should ideally include a representative highland and lowland site, a measurement in the volcanically active Tharsis province, and a determination of the mantle heat flow from a measurement in the Hellas basin. However, even a single measurement would be an extremely valuable addition to our knowledge of Mars.

Electromagnetic Sounding: Electromagnetic sounding has yielded important insights on the interior structures of the Moon and the Galilean satellites [38-40]. EM methods are widely used to understand Earth's structure from depths of meters to hundreds of kilometers. Objectives for Mars include the temperature and state of the upper mantle, the thicknesses of the lithosphere, crust, and cryosphere, and lateral heterogeneity in any of these properties. EM measurements are therefore complementary to seismology and heat flow in constraining the internal structure and evolution of Mars.

Time-varying EM fields induce eddy currents in planetary interiors, whose secondary EM fields are detected at or above the surface. These secondary fields shield the deeper interior according to the skin-depth effect, so that EM fields fall to $1/e$ amplitude over depth δ (km) = $0.5\sqrt{\rho/f}$, where ρ is the resistivity (in $\Omega\text{-m}$) and f is the frequency (in Hz). EM sounding exploits the skin-depth effect by using measurements over a range of frequency to reconstruct resistivity over a range of depth [41]. Natural EM signals (i.e., magnetospheric pulsations, ionospheric currents, lightning) are used instead of transmitters at the low frequencies necessary to penetrate kilometers to hundreds of kilometers into the Earth. Sources for Mars would likely include direct solar-wind/ionosphere interactions, diurnal heating of the ionosphere, solar-wind/mini-magnetosphere interactions, and possibly lightning. These sources would provide a spectrum from ~ 10 μHz (1 sol period) to >1 kHz.

Forward modeling of a variety of possible subsurface structures for Mars provides a broad mapping of measured frequency to depth of investigation. The cryosphere, from the surface to a depth of a few to tens of kilometers, is probably very resistive and hence EM-transparent. Underlying saline groundwater would be a near-ideal EM target. Grimm [42] shows that the depth to groundwater could be determined from measurements anywhere in the range of 1 mHz to 1 kHz. A wet crust would partly shield the deeper interior on Mars as on Earth, but, in both cases, frequencies of 1–100 μHz penetrate and are sensitive to

hundreds of kilometers depth. Higher frequencies (up to 100 mHz) penetrate to these depths if the crust is dry. There appears to be a good match, therefore, between the likely natural EM energy and the necessary investigation depths for the EM science objectives.

The fundamental quantity that must be derived is the frequency-dependent EM impedance Z . Two methods are suitable for constructing Z from measurements at the surface of Mars. Geomagnetic depth sounding uses surface arrays of magnetometers to determine Z from the ratio of the vertical magnetic field to the magnitude of the horizontal magnetic-field gradient [43]. Using this method, frequencies 10–100 μ Hz from ionospheric sources could be used to probe the mantle. The magnetotelluric method (MT) uses orthogonal horizontal components of the local electric and magnetic fields to compute Z . Mars MT would likely best apply to higher frequencies (<1 Hz to ~1 kHz) and hence exploit 0.01–1 Hz direct solar-wind/ionosphere interactions [44] as well as Schumann resonances (~10–50 Hz) and TM waves (>100 Hz) due to lightning. MT would therefore focus on the crust and cryosphere. Together, geomagnetic depth sounding and MT would address the MGN mission science goals.

Boundary Layer Meteorology: Although meteorological payloads on an interior-focused, two-lander network mission could not fully address the global measurements required to meet the highest priority Mars Exploration Program Advisory Group (MEPAG) climate goals and investigations [45], they could address important elements of the goal related to the dust, H₂O, and CO₂ cycles, as well as the behavior of trace gases that are exchanged with the surface. Specifically, a two-lander network mission could characterize the nature of surface-atmosphere interactions and how they vary in space and time. These interactions could only be determined from surface measurements rather than orbiters and have yet to be adequately characterized by any previous landed mission. The most important aspect of these interactions is the exchange of heat, momentum, water vapor, and trace species between the surface and atmosphere. Understanding these exchanges requires long-term, carefully calibrated, and systematic measurements of pressure, temperature, 3D winds, dust, water vapor, solar and infrared energy inputs, and the electrical environment. Such measurements, made at sufficiently high cadence and with some vertical discrimination, would yield quantitative estimates of the vertical turbulent fluxes of heat, mass, and momentum, which in turn would determine the surface forcing of the general circulation and the sources and sinks for dust, H₂O, and CO₂. Depending on how the network is configured, correlation studies could further help characterize the near surface signature of regional and larger-scale weather systems such as slope flows, baroclinic eddies, and thermal tides, especially if further supplemented with contemporaneous measurements from orbit.

Science Traceability

Table 1-1. Science Traceability Matrix

Science Objective	Measurement	Instrument	Functional Requirement
Characterize the internal structure of Mars to better understand its early planetary history and internal processes affecting its surface and habitability	Characterize crustal structure and thickness	VBB seismometer	<ul style="list-style-type: none"> At least one Mars year of continuous measurements 3-axis; noise floor better than $0.5 \times 10^{-9} \text{ m/s}^2/\text{Hz}^{1/2}$ from 2 mHz–5 Hz
	Investigate mantle compositional structure and phase transitions	X-band transponder	<ul style="list-style-type: none"> At least one Mars year of weekly measurements 0.1 mm/s for 60 s integration
	Characterize core size, density, state, and structure	EM sounder (passive)	<ul style="list-style-type: none"> 3-axis magnetometer: $0.01 \text{ nT/Hz}^{1/2}$ from 1 mHz–5 Hz; 0.1 nT DC 2-axis electrometer: $0.1 \text{ mV/m/Hz}^{1/2}$, 1 mHz–5 Hz
Characterize the thermal state of Mars to better understand its early planetary history and internal processes affecting the surface and habitability	Measure crustal heat flow	Mole with instrumented tether	<ul style="list-style-type: none"> At least one Mars year of daily measurements Temperature: 0.1 K relative precision at ≥ 10 points to 3 m depth Thermal conductivity: 10%
	Characterize thermal profile with depth	EM sounder (passive)	<ul style="list-style-type: none"> As above
Characterize the local meteorology and provide ground truth for orbital climate measurements	Measure the properties related to atmospheric thermodynamics and motion	Pressure sensor	<ul style="list-style-type: none"> 1–3 Pa accuracy at rates to 3 Hz
		Thermistors	<ul style="list-style-type: none"> 0.01 K accuracy at rates to 1 Hz over a range of height to >1 m
		Hot-wire anemometer	<ul style="list-style-type: none"> 2D speed and direction 10% accuracy from 0.1–100 m/s at rates to 1 Hz
		Acoustic anemometer	<ul style="list-style-type: none"> 3D speed and direction, vertical shear 10% accuracy from 0.1–100 m/s at rates to 8 Hz
		Humidistat	<ul style="list-style-type: none"> Better than $\pm 5\%$ accuracy at Mars ambient temperatures
		Electrometer	<ul style="list-style-type: none"> Quasi-DC E field from 10 V/m–10 kV/m AC field from 10 Hz–4 kHz with a sensitivity of 2 $\mu\text{V/m}$

Note: This matrix describes the linkages between science objectives and how they are achieved. Blue shading indicates the science floor objectives, measurements, instruments, and associated functional requirements. Note that the pressure sensor, thermistors, and hot-wire anemometer are defined as science floor instruments because they are required for the proper calibration of the seismometer. These atmospheric instruments also satisfy some of the meteorology science objectives, but as a whole, these objectives are not part of the baseline science of MGN.

2. High-Level Mission Concept

Overview

The mission system for the MGN mission would include two identical, independent flight systems. Each flight system would include three flight elements: a lander, an entry system, and a cruise stage. These elements would be combined in a Phoenix-like architecture. This architecture would focus the complexity on the lander element, and allow the cruise stage and entry system to remain as simple as possible.

September 2022 was used as the nominal launch date for this study followed by cruise durations of ~6 months. For launch, the flight systems would be stacked vertically with a dual-payload adapter supporting the upper flight system, and the lower flight system attached directly to the Centaur upper stage of the launch vehicle. Shortly after launch, the two spacecraft would be released within hours of each other. The upper stage would provide the delta-V necessary to achieve a seven-day separation for arrival at Mars.

Just prior to entry, the entry system (including the lander) would separate from the cruise stage, which would proceed to burn up in the martian atmosphere. The entry system would use an aeroshell and parachute for initial deceleration. The heatshield would be subsequently jettisoned and the lander would descend the final ~1,000 m to the surface using powered descent engines. A landing radar and inertial measurement unit (IMU) would provide the needed attitude, velocity, and altitude knowledge to allow for safe landing. The entire EDL sequence would be repeated by the second entry and landing system seven days after the first.

Initial surface operations would include deployments of the lander solar array, robotic arm, and atmospheric instrument suite (ATM) mast, followed by placement of the seismometer on the surface. Once the seismometer is deployed, the robotic arm would not need to be used again for the remainder of the mission, and there would be no further tactical operations. Each lander would then operate continuously as a simple monitoring station with routine operations.

Science data would be relayed twice daily from each lander via ultra-high frequency (UHF) to an existing orbiting asset. Downlink to Earth would be based on the asset's Deep Space Network (DSN) schedule. The data volume for the entire mission duration of one martian year would be less than 40 Gbytes. The ground data system would be relatively simple and the science team would be small.

Concept Maturity Level

Table 2-1 summarizes the NASA definitions for concept maturity levels (CMLs). Based on an assessment of the results of this study, this concept is considered to be at CML 4. The architecture studied was defined at the assembly level based on previous Team X studies with estimates developed for mass, power, data volume, link rate, and cost using JPL's institutionally endorsed design and cost tools. Risks were also identified and assessed as to their likelihood and mission impact, as discussed later in the report.

Table 2-1. Concept Maturity Level Definitions

Concept Maturity Level	Definition	Attributes
CML 6	Final Implementation Concept	Requirements trace and schedule to subsystem level, grassroots cost, V&V approach for key areas
CML 5	Initial Implementation Concept	Detailed science traceability, defined relationships, and dependencies: partnering, heritage, technology, key risks and mitigations, system make/buy
CML 4	Preferred Design Point	Point design to subsystem level mass, power, performance, cost, risk
CML 3	Trade Space	Architectures and objectives trade space evaluated for cost, risk, performance
CML 2	Initial Feasibility	Physics works, ballpark mass and cost
CML 1	Cocktail Napkin	Defined objectives and approaches, basic architecture concept

Technology Maturity

No technology development would be required for this mission. This is largely in keeping with the initial design goal of consistency with New Frontiers competitive missions. MGN leverages powered descent, landing radar, and robotic arm heritage from previous Mars missions including Phoenix. Key technology development for the seismometer has been conducted over the past two decades, culminating in a TRL 5–6 instrument developed for the ESA ExoMars mission as part of the Humboldt package. The baseline atmospheric instruments are all high TRL and have heritage from the Pathfinder, Mars Polar Lander (MPL), and Phoenix missions.

Key Trades

Landing Architecture

The landing architectures considered in this study included powered descent landers similar to the Phoenix and Viking missions, and airbag landers similar to the MPF and Mars Exploration Rover (MER) missions. The advantages of a powered descent system include the ability to utilize a single integrated propulsion system for the lander and cruise stage, lower flight system mass, larger volume (and mass) available for payload, and the ability to accommodate larger landed solar arrays. The main advantages of an airbag lander include the robustness of the landing approach and lower recurring flight system costs. After a high-level architectural assessment of these two architectures in a previous Decadal Study effort [1], it was found that the powered lander approach is more cost effective for a two-node geophysical network mission. Therefore, it was chosen as the baseline for the MGN mission.

Launch Configuration

Two launch configurations were considered in this study. Historical Mars-surface spacecraft have been launched in a horizontal configuration as shown in Figure 2-1. Since this mission would involve two landers, a stacked configuration as shown in Figure 2-2 would be most analogous to historical launch configurations. The drawback to a stacked configuration would be the risk of separation failure of the first vehicle, resulting in the inability to separate the second. This risk could be mitigated by employing a vertical configuration as shown in Figure 2-3.

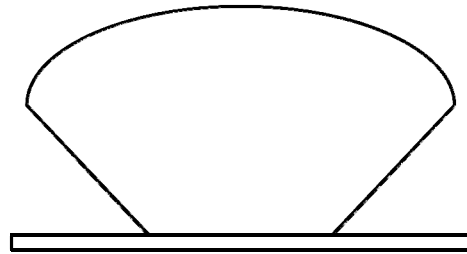


Figure 2-1. Typical Orientation for Mars Surface Spacecraft

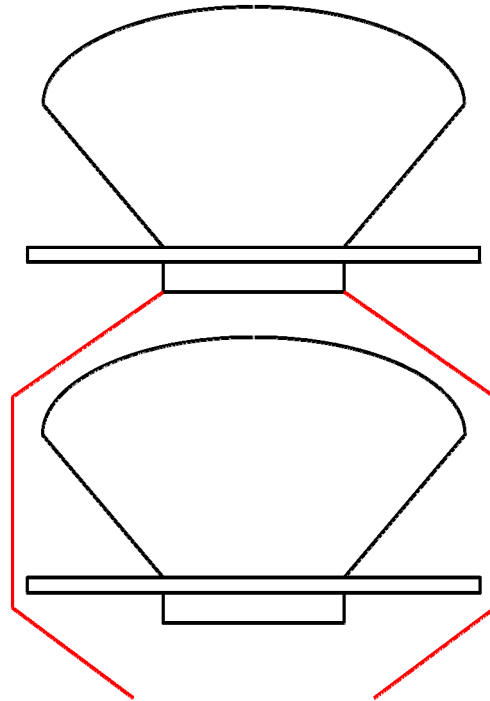


Figure 2-2. Concept of a Two-Lander Stacked Configuration

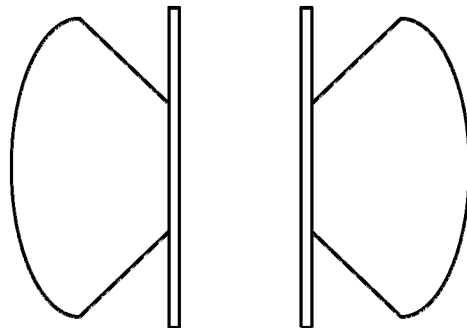


Figure 2-3. Concept of a Two-Lander Vertical Configuration

Since the launch vehicle thrust direction would impart axial loads on the spacecraft in the vertical configuration, each of the spacecraft would need to be designed to accommodate higher launch loads than historical missions. Changing the primary load path of the spacecraft would cause any heritage to historical missions to be lost. This design would require significantly higher structural mass to stiffen the spacecraft.

The vertical configuration would be subjected to an additional guidance, navigation, and control (GNC) design problem. It is quite common for the Earth-Mars Type I/II interplanetary trajectory to achieve the targeted C3 with only two Centaur upper stage burns. However, if the MGN mission releases the first spacecraft at the end of the second Centaur burn and performs an attitude control change with reaction control system (RCS) thrusters prior to the third Centaur burn and second spacecraft release, a new GNC algorithm/thruster location would need to be developed in order to accommodate a substantial center of gravity (CG) offset in the dispenser-spacecraft Centaur configuration. Currently, the feasibility of such a design is uncertain.

Another option for the vertical configuration design would be to not rely on the third Centaur burn as an additional maneuver for the required arrival conditions on Mars (i.e., seven days apart between the two EDLs). In this case, upon reaching the hyperbolic injected state, the two spacecraft would be simultaneously separated and would reorient their attitude and perform a necessary ΔV maneuver. Each lander would perform the separation maneuver in opposite directions, one to delay Mars arrival by ~3.5 days and another to accelerate Mars arrival by 3.5 days. Together, these maneuvers would provide the desired seven-day separation between the arrivals at Mars. However, this approach would lead to an increase in the propellant tank size carried by each spacecraft relative to the baseline (stacked) configuration in which the third burn of the Centaur upper stage would provide the needed separation delta-V.

Moreover, the vertical configuration would require a 5 m faring for the Atlas V class of launch vehicles. This would result in a cost increase and establish a lower C3 versus injected mass capability. For the Earth-Mars 2022 opportunity, the MGN launch mass would exceed the capability of the Atlas V 501 on a Type I trajectory. This would force the mission design to a longer 400-day Type II transfer that would result in increased costs for mission operations system (MOS), ground data system (GDS), DSN, science, and navigation. Alternatively, a more capable and more costly launch vehicle (Atlas V 511) could be used with the baseline Type I trajectory.

After considering all aspects of both the stacked and vertical configurations, the stacked design would require less development and was therefore chosen for this mission.

Cruise Stage Architecture

During the previous Decadal Survey trade study effort, options for the cruise stage architecture were considered. One approach would be to utilize a “common carrier” that would deliver the combined entry systems/landers to Mars with a single cruise stage/carrier element. Though this architecture would eliminate the need for the two simple cruise stages and the dual payload adapter, it would require a more complex carrier flight element that must still support the combined mass of each entry system and lander during launch, and be able to release them shortly before Mars arrival. This approach was ultimately rejected in favor of the baseline (“free flyer”) architecture due to issues associated with achieving the desired entry separation. The most significant challenge was the entry system design required to meet the power and thermal needs of the lander during detached cruise without solar power. The addition of body-fixed solar cells to the exterior of the backshell was considered, but the additional cost and complexity were thought to outweigh the savings achieved through the elimination of the simple cruise stages. The option of relaxing the entry separation from seven days down to a few hours was also considered, but the increased risk during EDL was deemed unacceptable. The primary concern was the stress on the mission operations system and the inability to react to anomalies encountered during the EDL sequence of the first lander.

3. Technical Overview

Instrument Payload Description

The instrument payload for the MGN mission would be consistent with the baseline science described in Section 2. The instruments that comprise this payload include the seismometer (SEIS), instrument deployment arm (IDA), instrument deployment camera (IDC), stereo cameras, atmospheric instrument suite (ATM) and X-band transponder. The baseline ATM is made up of temperature and pressure sensors and a hot-wire anemometer. The precision tracking experiment is also included in the MGN point design, though the hardware needed to conduct this experiment is part of each lander’s telecommunications subsystem.

Secondary science instruments, such as a heat flow probe (HP³), dust opacity and concentration instruments, an electromagnetic sounder (EMS), a humidistat, and sonic anemometer instruments are not included in the MGN point design and are not needed to meet the baseline science objectives. However, if there were sufficient resources to include these instruments they would provide considerably enhanced science directly addressing the goals of the mission. Thus, descriptions of these optional instruments are included below. The impact on the flight system caused by the addition of the secondary science instruments has not been fully evaluated, but is expected to be minimal. For example, the Phoenix mission flew with a science payload of approximately 60 kg, but the current MGN payload is only 25 kg (CBE + 30% contingency).

Table 3-1 provides the mass and power details for the baseline instrument payload.

Table 3-1. Payload Mass and Power

	Mass			Average Power		
	CBE (kg)	% Cont.	MEV (kg)	CBE (W)	% Cont.	MEV (W)
Seismometer	6	33%	8	1.8	33%	2.4
IDA (robotic arm)	5	40%	7	28	43%	40
IDC (Navcam)	0.22	50%	0.33	2.2	36%	3
Stereocams (2)	0.44	50%	0.66	4.4	36%	6
ATM (P,T, W)	1.5	67%	2.5	2	50%	3
Total Payload Mass	13.2	40.5	18.5	38.4	41.7	54.4

Seismometer

The seismometer described below is based on a design that has been offered by an international collaboration on numerous previous NASA mission concepts and proposals dating from the mid-90s to the present. The most current configuration of the seismometer encompasses hardware from France (Institut de Physique du Globe de Paris), the United Kingdom (Imperial College, London), Germany (Max Planck Institute, Lindau), Switzerland (Swiss Federal Institute of Technology, Zurich), and the US (Jet Propulsion Laboratory, Pasadena). The instrument relies on the ExoMars Geophysical Package (GEP) development that was based on the NetLander Phase B development, which in turn built on the foundation of the OPTIMISM experiment for the Mars’96 mission. It is the subject of continuing development for use on the Moon by the Japanese SELENE-2 mission.

This instrument was chosen for the study because it is the only design currently available that fulfills the demanding science measurement requirements and is compatible with planetary flight and operational requirements. Although it is largely a non-US development, it has been assumed that the cost of building the hardware would be borne by NASA. This is possible because although the components of the instrument are developed by various European research institutes, the institutes do not fabricate flight

instruments but rather contract them to industry. The estimated cost for this approach is the anticipated industrial contract cost based on information supplied by the European developers. This approach is the baseline assumed for the MGN mission concept.

Two other acquisition options are possible. The first would be a contribution by the European agencies responsible for the development (CNES in France, DLR in Germany, the UK Space Agency, and CFAS/PRODEX in Switzerland). There is a long-standing collaboration among European and US investigators that has led to such contributions being endorsed for many NASA proposals (and US contributions being endorsed for ESA proposals), so this option is considered quite plausible.

The second alternative would be a US-only development. It would be necessary to take a classical terrestrial very broad band (VBB) seismometer with the required performance, decrease its mass and power requirements, and qualify it for flight loads, radiation, and Mars surface temperature conditions. For example, a Streckeisen STS-2 is one of the few terrestrial VBB sensors with the required performance. It weighs approximately 9 kg, requires approximately 1.2 W for the sensor, and has already been operated in Antarctic conditions below -50°C . (Note however that even terrestrial seismology is a very international undertaking. Streckeisen is a Swiss company, although it is owned by Kinemetrics in the US. The US dense seismological network set up by IRIS uses exclusively European broad band sensors, either from Streckeisen of Switzerland or Guralp of the UK.) The ~ 10 -year VBB technology development program in France has led to a reduction of the mass by a factor of 3–4 and of the power by a factor of 2–3, while making the instrument compatible with g-loads of 200 g. It is estimated that it would take \$10–15M (FY10) and approximately 4 years for a US team to develop a comparable VBB instrument based on an existing terrestrial design, perhaps with more modest mass, power, and shock resistance improvement goals. SP sensors are currently available that would require modest development for flight qualification. The acquisition electronics are also relatively standard and are comparable to the acquisition electronics of a magnetometer, for which US expertise is available.

Instrument Description: The SEIS instrument is composed of an evacuated sphere assembly, enclosing three VBB orthogonal oblique seismometers, along with three additional independent orthogonal short period (SP) seismometers outside the sphere. The sphere is thermally decoupled from the environment by an insulated wind cover. The sphere also encloses a set of secondary sensors (temperature and inclination) used for both instrument management and scientific purposes. Pressure sensors are both inside (for monitoring the vacuum quality) and outside (for monitoring atmospheric pressure changes) the sphere. The external pressure sensor is sampled at 20 Hz to cover the infrasonic range. The VBB seismometer has been under development by IPGP since the late 1980s and the SP was developed first by JPL and later by Imperial College since the mid-90s.

The seismometer noise power spectral density, which defines the noise floor of the instrument, is shown in Figure 3-1. Figure 3-2 provides the response and noise curves for the seismometer. It meets the mission requirements for the VBB seismometers ($<10^{-9} \text{ m/s}^2/\text{Hz}^{1/2}$ from 10^{-3} –2 Hz) and the SP seismometers ($<10^{-8} \text{ m/s}^2/\text{Hz}^{1/2}$ from 5×10^{-2} –100 Hz). The SP seismometer is sampled at a selectable rate between 20 and 200 Hz and the VBB seismometer is sampled at a selectable rate between 2 and 20 Hz. Details of the SEIS are provided in Table 3-2.

The IDA would deploy the seismometer package from its stowed position on the lander onto the surface of Mars. A tether would provide power and data connection between the SEIS and the warm electronics module (WEM). Three fixed, pointed feet on the bottom of the seismometer would aid high frequency coupling to the martian soil. The instrument would be fully operational after its initialization sequence (i.e., leveling, pendulum centering, and feedback tuning). This sequence and the subsequent calibration activity, which consists of monitoring the temperature impact on the instrument in order to set the thermal loop compensation, would last several weeks. The SEIS instrument including the leveling mechanism was at TRL 6 and passed PDR for the ExoMars mission before being descoped. Recent changes to the system have reduced the TRL to 5, however there is an existing funded plan to return to TRL 6 by the fall of 2010. The development is being funded by CNES, for use on the Japanese SELENE-2 mission.



Figure 3-1. SEIS showing the evacuated sphere where the VBB sensors are located, the base, and support structure.

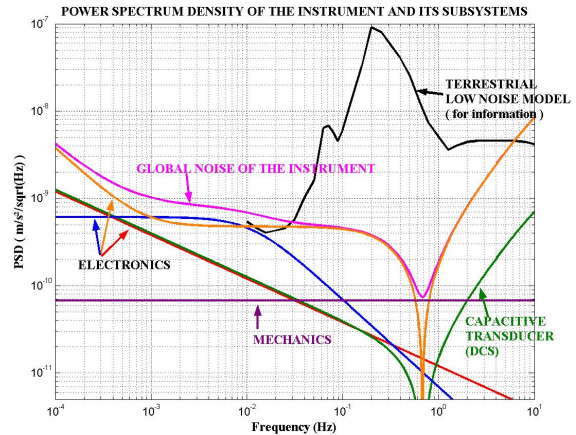


Figure 3-2. Response and noise curves for the seismometer.

Table 3-2. SEIS

Item	Value	Units
Type of instrument	Seismometer	
Number of channels	>20	
Size/dimensions (for each instrument)	0.3 h x 0.4 dia	m x m x m
Instrument mass without contingency (CBE*)	6	kg
Instrument mass contingency	33%	%
Instrument mass with contingency (CBE+Reserve)	8	kg
Instrument average power without contingency	1.8	W
Instrument average power contingency	33%	%
Instrument average power with contingency	2.4	W
Instrument average science data rate [^] without contingency	8	kbps
Instrument average science data [^] rate contingency	31%	%
Instrument average science data [^] rate with contingency	10.5	kbps
Sensitivity	<10 ⁻⁹ m/s ² Hz ^{-1/2} from 10 ⁻³ to 10 Hz <10 ⁻⁸ m/s ² /Hz ^{1/2} from 5×10 ⁻² –100 Hz	
Instrument fields of view (if appropriate)	N/A	degrees
Pointing requirements (knowledge)	1	degrees
Pointing requirements (control)	N/A	degrees
Pointing requirements (stability)	N/A	deg/sec

*CBE = Current best estimate

[^]Instrument data rate defined as science data rate prior to on-board processing

Instrument Deployment Arm

The requirements for the IDA are to provide access to a range of at least 2 m and 150° on terrain slopes of up to 15° for placement of the seismometer. The IDA described here meets all requirements and is a Phoenix-derived design, but with reduced linked lengths and brushless motors. It has 4 DOF (i.e., shoulder yaw and pitch, elbow and wrist pitch). Each of the four actuators carries a temperature sensor and heater and uses a potentiometer for broad position determination and a magnetoresistive relative-count encoder for precise motion determination. The IDA carries an end-effector on the wrist joint (Figure 3-3). Based on a “crow’s foot and grapple” approach, this simple design allows for reliable instrument manipulation even with maximum IDA positioning error (5 mm close to the arm base, 2 cm when fully extended). The concept was brought to critical design review (CDR)-level during the Mars Surveyor’01 project planning phase and was tested on slopes up to 16°.

As each instrument is deployed, a cable box would passively pay out the umbilical tethers that connect the instrument to the WEM electronics and power supply. The cables would be in an accordion pleat configuration inside the boxes and would be strong, flexible, and strain relieved.

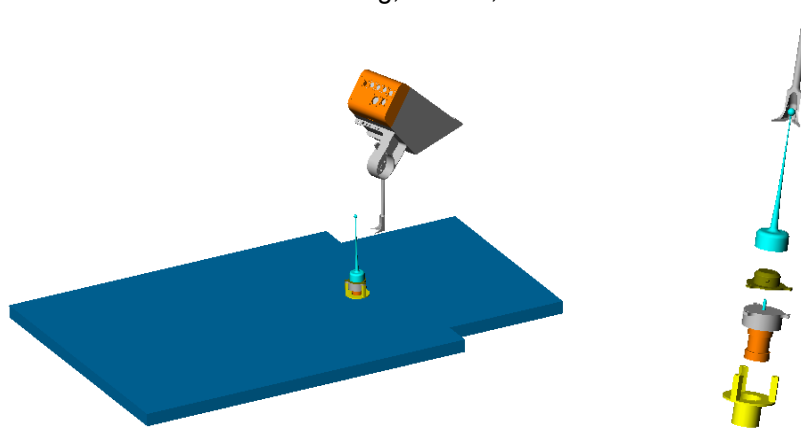


Figure 3-3. IDA end effector and ball-on-stalk device for picking up and placing SEIS on the ground.

Camera Systems

The purpose of the camera system is to support seismometer deployment. It consists of an Instrument Deployment Camera (IDC) and a pair of Stereocams. The IDC, which has MER Navcam heritage (Figure 3-4), would be attached to the forearm of the IDA and would be used for imaging deployments. It could also be used to study the surrounding geology and perform atmospheric dust opacity measurements. Two Stereocams based on the MER Hazcams would be fixed to the lander and would provide stereo images of the work area reachable by the IDA. The IDC would be fitted with a set of filters of the same design as the Pancam in order to monitor dust opacity. Technical interface details for the cameras are provided in Tables 3-3 and 3-4.



Figure 3-4. Navcam Camera on Which the IDC Would be Based

Table 3-3. Instrument Deployment Camera

Item	Value	Units
Type of instrument	Camera	
Number of channels	1	
Size/dimensions (for each instrument)	0.04 x 0.05 x 0.02	m x m x m
Instrument mass without contingency (CBE*)	0.22	kg
Instrument mass contingency	50%	%
Instrument mass with contingency (CBE+Reserve)	0.33	kg
Instrument average power without contingency	2.2	W
Instrument average power contingency	36%	%
Instrument average power with contingency	3	W
Instrument average science data rate [^] without contingency	2,000	kbps
Instrument average science data [^] rate contingency	25%	%
Instrument average science data [^] rate with contingency	2,500	kbps
Sensitivity	0.76	mrاد/pixel
Instrument fields of view (if appropriate)	N/A	degrees
Pointing requirements (knowledge)	N/A	degrees
Pointing requirements (control)	N/A	degrees
Pointing requirements (stability)	N/A	deg/sec

*CBE = Current best estimate

[^]Instrument data rate defined as science data rate prior to on-board processing

Table 3-4. Stereocams (Two)

Item	Value	Units
Type of instrument	Camera	
Number of channels	1	
Size/dimensions (for each instrument)	0.04 x 0.05 x 0.02	m x m x m
Instrument mass without contingency (CBE*)	0.22	kg
Instrument mass contingency	50%	%
Instrument mass with contingency (CBE+Reserve)	0.33	kg
Instrument average power without contingency	2.2	W
Instrument average power contingency	36%	%
Instrument average power with contingency	3	W
Instrument average science data rate [^] without contingency	2,000	kbps
Instrument average science data [^] rate contingency	25%	%
Instrument average science data [^] rate with contingency	2,500	kbps
Sensitivity	1.2	mrاد/pixel
Instrument fields of view (if appropriate)	N/A	degrees
Pointing requirements (knowledge)	N/A	degrees
Pointing requirements (control)	N/A	degrees
Pointing requirements (stability)	N/A	deg/sec

*CBE = Current best estimate

[^]Instrument data rate defined as science data rate prior to on-board processing

X-Band Transponder

The X-band transponder would be the same hardware used by the spacecraft for communication with Earth during cruise. No data would be collected on Mars. The transponder must be on for 1 hour per week for the duration of the mission. The transponder requires 43 W of power when it is operational. It may be possible to turn off the main amplifier for much of the tracking pass and only transmit back to Earth at the beginning and end of the pass. The receiver on Mars would have to accumulate phase during the time between transmissions. If this power saving technique were used, the power requirement would drop to 19 W during the non-transmitting period.

Atmospheric Instruments

The atmospheric instruments would be mounted on a 1.2 m tall mast, which would use spring action to deploy itself to an attitude perpendicular to the lander deck when the latch is released. The instruments would consist of pressure and temperature sensors, and an anemometer. Technical details of the ATM are provided later in this section in Table 3-5.

Atmospheric Pressure

An atmospheric pressure gauge would be housed in the WEM with a 2 mm diameter port to the atmosphere. The sensor would have an absolute accuracy of 1–3 Pa throughout the range of pressures anticipated on the martian surface (500–1,200 Pa). The output would consist of a 4–12 kHz signal monitored by a 10 MHz counter, providing a resolution of ~25 mPa for an integration time of 1 sec. This sampling rate and resolution would resolve rapid (1–10 sec) small-amplitude (1–3 Pa) pressure disturbances like those associated with dust devils.

The mission would use a Vaisala Barocap pressure sensor like those developed and tested for the MPL Mars Volatiles and Climate Surveyor (MVACS) instrument suite and the Phoenix Scout mission. This pressure sensor has a mass of 45 gm and dimensions of 60 × 40 × 25 mm and requires <100 mW for continuous operations. A single pressure sample (including housekeeping data) requires 384 bits. If this is sampled at 3 Hz for 5-minute periods every half hour, the data volume would be 14.4 Mbit/sol.

Atmospheric Temperature

Thermocouples (TCs) to measure the atmospheric temperature would be mounted at 0.25, 0.5, and 1.0 m above the base of the mast. Another pair of sensors would be deployed on the ground. The reference junctions for the TCs would be located on an isothermal block (IB), whose temperature is recorded by a precision platinum resistance thermometer (PRT). The TCs have been used in previous Mars landers and would be built by JPL. The IB and its PRT would be incorporated into the base of the wind sensor at the top of the ATM mast.

Each TC assembly has a mass of <10 gm and dimension of 30 × 45 × 2 mm. The total system requires <90 mW for continuous operation. To resolve rapid temperature variations, TCs must be sampled at 0.2–1 Hz. A single temperature sample includes the five TCs, the IB PRT, and one reference (zero point) TC mounted on the IB PRT. Each measurement is recorded as a 16-bit word. If the sampling rate is 1 Hz, the data rate would be 128 bits per second (bps). If samples are collected for 5 minutes every 30 minutes, the total data volume would be 2.64 Mbit/sol.

Hot-wire Anemometer

The horizontal wind velocity at the top of the mast would be monitored by a directional hot-wire anemometer. Its configuration and principle of operation are shown in Figure 3-5. The MVACS-derived control circuit maintains the hot wire at 100°C above ambient atmospheric temperature, and the wind speed is determined by measuring the power needed to maintain the hot wire at this temperature. The wind sensor circuit uses ambient atmospheric temperature measurements from a pair of TCs that are mounted between the wind sensor support disks, just outside of the direction TCs. The two TC arrays are mounted 180° apart so that one is always upstream, uncontaminated by the warm plume.

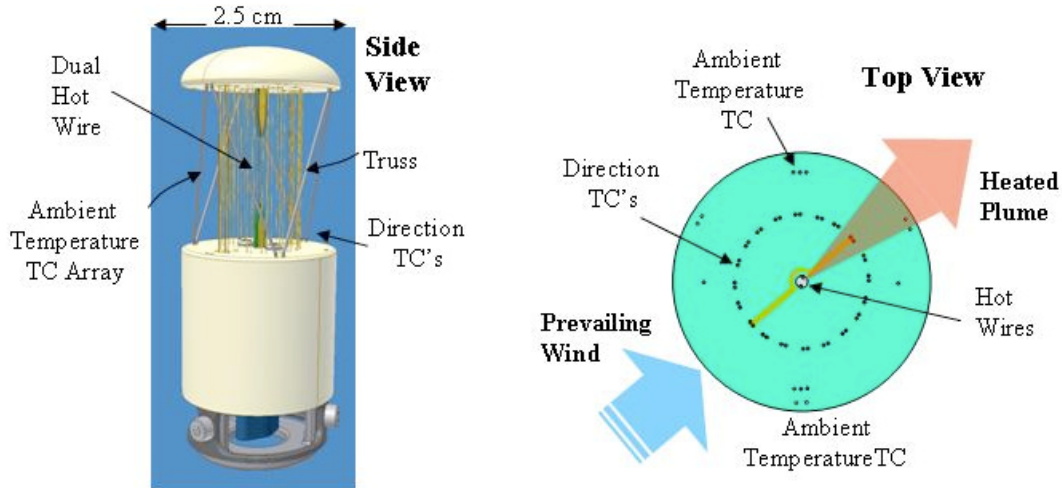


Figure 3-5. Hot-wire Anemometer Details and Operational Principle

The direction of the heated plume from the sensor's hot wires is detected by an array of 20 TCs surrounding the hot wires, which yield a directional resolution of $\pm 9^\circ$. These TCs are identical to those used to sense the atmospheric temperature, but are connected so that they measure the temperature difference between opposite sides of the hot wire instead of the ambient temperature.

The wind velocity sensor uses a pair of hot-wire elements connected in parallel to provide redundancy. The hot wires are supported on tapered posts that are inserted through the centers of a pair of 1 mm thick fiberglass disks that form the top and bottom of the sensor, separated by a truss consisting of six 0.5 mm stainless steel wires. This disk-truss structure provides support and introduces minimal dynamical obstruction or thermal contamination.

The wind velocity sensor has a mass of 30 gm and dimensions of $25 \times 25 \times 75$ mm, and requires 300 mW for continuous operation. Like temperatures, wind velocities must be sampled at 0.2–1 Hz to resolve convection, dust devils, and other rapidly varying phenomena. Each wind sample includes the hot-wire voltage and current, two ambient TCs, and 10 outputs from the directional TCs.

When each of these 14 values is digitized with a 16-bit ADC and sampled at 1 Hz, the raw data rate is 224 bps. If the wind direction is determined on board, the data rate falls to 80 bps. For this case, if data is collected for 5-min periods at 1 Hz every 30 minutes, the total data volume would be 1.2 Mbit/sol.

For MPL-MVACS, extensive tests were conducted in the Mars Aeolian Facility at NASA Ames (with blowing dust) and in Mars chambers at JPL. These tests confirmed that the instrument was both robust and reliable, producing accuracies of $\sim 10\%$ at wind speeds between 0.1 and 100 m/s at Mars-like pressures and temperatures. The MVACS wind velocity sensor survived 600 g's in pre-flight testing.

Table 3-5. ATM (P, T, W)

Item	Value	Units
Type of instrument	Meteorology package	
Number of channels	20	
Size/dimensions (for each instrument)	0.1 x 0.1 x 0.1	m x m x m
Instrument mass without contingency (CBE*)	1.5	kg
Instrument mass contingency	67%	%
Instrument mass with contingency (CBE+Reserve)	2.5	kg
Instrument average power without contingency	2	W
Instrument average power contingency	50%	%
Instrument average power with contingency	3	W
Instrument average science data rate [^] without contingency	9.6	kbps
Instrument average science data [^] rate contingency	35%	%
Instrument average science data [^] rate with contingency	13	kbps
Sensitivity	P=1–3 Pa, T=0.1 K, W=0.1 m/s	–
Instrument fields of view (if appropriate)	N/A	degrees
Pointing requirements (knowledge)	N/A	degrees
Pointing requirements (control)	N/A	degrees
Pointing requirements (stability)	N/A	deg/sec

*CBE = Current best estimate

[^]Instrument data rate defined as science data rate prior to on-board processing

Potential Additional Instruments

The following instruments are not in the baseline MGN design, but could potentially be added to MGN if budget were available and accommodation on the lander were possible. There is a possibility that a heat flow probe could be contributed by DLR. Contributions of instruments needed to meet the threshold science could potentially make additional budget available for other secondary science instruments. For example, there is a possibility that a heat flow probe could be contributed by DLR.

Geophysical Instruments

Heat Flow Probe

A heat flow probe (HP³) would penetrate a substantial thickness (≥ 3 m) of the regolith of Mars while trailing a tether carrying thermal sensors to measure martian heat flow. Additional data delivered by the instrument would describe thermophysical and strength properties of the regolith to investigate local stratigraphy, and soil dielectric properties that are diagnostic of small concentrations of water or ice that might be present in the regolith.

The IDA would deploy the heat flow unit from its stowed location on the lander to the surface of Mars. A tether would provide the power and data connection between the heat flow unit and the WEM.

At the core of the HP³ system is an electromechanical penetrometer (mole) that would travel downward into the regolith by soil displacement through the action of an internal hammering mechanism. Impacts from the mechanism would accelerate the mole forward while the recoil force is reacted by wall friction to the surrounding soil, allowing net forward motion. Depths of several meters might be reached in cumulative operating durations of a few hours, depending on soil compaction properties. The instrumented mole consists of a leading compartment (tractor mole) housing the electromechanical hammering mechanism and a payload compartment (trailer mole) with a short flexible link connecting the two.

This two-body configuration has an advantage over a “monolithic” mole in that the two units can be stored perpendicularly to one another, offering a compact stowage configuration. The two-body configuration also allows the tractor mole to deflect through a wider angle around an obstruction.

The HP³ would be supplied by the DLR and is a version of the HP³ developed by DLR for BepiColombo and ExoMars. The tractor mole is based on the Planetary Underground Tool (PLUTO) flown on Beagle-2. The two-body HP³ has been under development since 2003.

The tractor mole carries a suite of sensors that monitor the acceleration and tilt of the mole. The depth of penetration can be calculated from the integrated acceleration and deflection from vertical. However, errors accumulate quickly with depth; therefore, the payout of the tether would be monitored for a better depth measurement.

Given the known impulse of the hammer, the force and reaction of the device allow the measurement of the resistance of the soil, resulting in a measure of the soil mechanical properties.

Thermistors are embedded in the tether and would be used to monitor the temperature gradient in the hole every hour for one full Mars year. There would be 20 thermistors providing 16 bits/hr for an average data rate of 8 kbit/sol.

The tether is made of multiple layers of kapton with a layer of thin copper conductors. It has been designed to provide a poor thermal conduction route in order to minimize the effect of the tether on the measurement. A mini-WEM attached to the HP³ housing would contain electronics for reading the thermistor outputs.

The mole has heaters so that it can monitor the temperature rise and decay of the surrounding soil in response to a heat pulse. These measurements would be used to infer the thermal conductivity of the material with depth. Based on expected regolith properties, the hole is expected to remain open after penetration. It is essential that the air in the hole not be disturbed. For that reason, the IDA would hold the surface unit in position while the mole is operating to seal the top of the hole. The unit would have outriggers that would steady it after the IDA is removed. Details of the HP³ are provided in Table 3-6.

Table 3-6. HP³

Item	Value	Units
Type of instrument	Heat flow probe	
Number of channels	40	
Size/dimensions (for each instrument)	0.35 x 0.28 x 0.22	m x m x m
Instrument mass without contingency (CBE*)	1.5	kg
Instrument mass contingency	33%	%
Instrument mass with contingency (CBE+Reserve)	2	kg
Instrument average power without contingency	2.6	W
Instrument average power contingency	35%	%
Instrument average power with contingency	3.5	W
Instrument average science data rate [^] without contingency	0.002	kbps
Instrument average science data [^] rate contingency	1525%	%
Instrument average science data [^] rate with contingency	0.036	kbps
Sensitivity	0.005	K precision
Instrument fields of view (if appropriate)	N/A	degrees
Pointing requirements (knowledge)	N/A	degrees
Pointing requirements (control)	N/A	degrees
Pointing requirements (stability)	N/A	deg/sec

*CBE = Current best estimate

[^]Instrument data rate defined as science data rate prior to on-board processing

Electromagnetic Sounder

The EMS would measure the subsurface electrical conductivity from 100 m to 100 km depth. The temperature structure and depth to or absence of groundwater could be inferred from the EMS measurements.

The EMS consists of two electrodes that must make electrical contact with the ground. The electrodes are on the end of two 2 m long booms that are deployed at right angles to each other or at the end of 20 m long ribbon cables that are deployed ballistically with spring-loaded bobbins. Two magnetometers per lander would be used to monitor magnetic fields.

The EMS is a passive instrument that uses ambient EM energy to probe the electrical properties of the outer layers of Mars. It has the greatest penetration of any method other than seismology. Magnetotellurics and geomagnetic depth sounding could be inverted for electrical conductivity as a function of depth. This in turn could be combined with laboratory measurements to constrain the temperature and composition of the subsurface materials.

The data rate would be 5–10 Mbit/sol, the mass is estimated to be 2.3 kg, and the power required is estimated to be 3.9 W. The required sensitivity is 10 pT/sqrt(Hz), 100 μ V/m/sqrt(Hz) at 1 Hz. The cost is estimated to be \$8M. Further details can be found in Table 3-7.

Table 3-7. Electromagnetic Sounder

Item	Value	Units
Type of instrument	Electromagnetic sensor	
Number of channels	15	
Size/dimensions	two 0.2 x 0.2 x 0.1 (stowed) probes, one 3U electronics board	m x m x m
Instrument mass without contingency (CBE*)	4	kg
Instrument mass contingency	38%	%
Instrument mass with contingency (CBE+Reserve)	5.5	kg
Instrument average power without contingency	3.9	W
Instrument average power contingency	41%	%
Instrument average power with contingency	5.5	W
Instrument average science data rate [^] without contingency	0.057	kbps
Instrument average science data [^] rate contingency	100%	%
Instrument average science data [^] rate with contingency	0.115	kbps
Sensitivity	1 pT/sqrt(Hz), 100 uV/m/sqrt(Hz) @ Hz	
Instrument fields of view (if appropriate)	N/A	degrees
Pointing requirements (knowledge)	N/A	degrees
Pointing requirements (control)	N/A	degrees
Pointing requirements (stability)	N/A	deg/sec

*CBE = Current best estimate

[^]Instrument data rate defined as science data rate prior to on-board processing

Atmospheric Instruments

Sonic Anemometer

A sonic anemometer would measure the 3D wind velocity at the top of the mast. Its configuration is shown in the Figure 3-6. The instrument would consist of six sound transducers arranged in pairs along three mutually orthogonal axes. The flight time of sound between opposing pairs of sensors (+ and – velocity along 3 axes = 6 directions) would be measured and used to solve for the 3D wind velocity vector.

Coupling between the sonic sensor/actuator and the atmosphere at Mars requires a different transducer compared to Earth due to the low atmospheric pressure (Mars $\leq 0.6\%$ Earth). An electrostatic transducer is available and has been tested to operate under Mars-like conditions of pressure, temperature, and dust.

The advantages of the sonic anemometer over the hot-wire anemometer flown on previous missions is the ability to measure the 3D wind vector compared to the horizontal 2D wind vector and the ability to operate at 8 Hz or higher while the response time of the TCs and heater wire limits the hot-wire anemometer to around 1 Hz.

The mass of the instrument would be 1.0 kg with an average power of 3.0 W. The data rate would be 9.6 kbits/sec in the worst case.

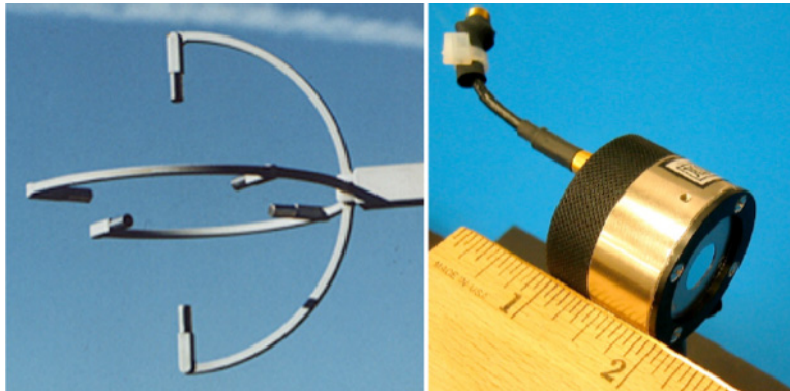


Figure 3-6. Sonic anemometer (left) and a photograph of the electrostatic transducers that enable sonic anemometry at Mars (right).

Atmospheric Humidity

In-situ measurements of the near-surface humidity would be made with a Vaisala Humicap sensor contributed by the Finnish Meteorological Institute (FMI). It would be mounted 0.5 m above the base of the mast. Humicaps sensors would determine the humidity as water vapor is adsorbed in a polymer sandwiched between capacitive electrodes. They typically have accuracies of $\pm 3\%$ relative humidity at temperatures between 190–350 K. They work at lower temperatures, but their response time increases from 5 minutes to >30 minutes as temperature decreases from 200 K to 170 K. The MSL REMS “Digihum” implementation, which includes the Humicap sensor and the electronics for digitizing the Humicap data has been baselined. Because the Digihum sensor head would be exposed to the Mars environment, it has been qualified from 150–290 K. The output of these sensors would be identical to that of the Barocap pressure sensors described above. It consists of a frequency signal between 3 and 20 kHz that is monitored by a 10 MHz counter. This frequency data would be read by the electronics board in the WEM.

The humidity sensor has a mass of 16 gm and dimensions of $16 \times 16 \times 35$ mm, and requires <100 mW for continuous operation. A single humidity sample (including housekeeping data) requires 384 bits. If the humidity is measured twice an hour throughout the sol, the total data volume would be 19.2 kbit/sol.

Dust Opacity

As on Viking, MPF, and MER, the total column dust optical depth could be monitored by direct observation of the Sun through special solar filters on the IDC. In order to do this, the IDC would be outfitted with a set of filters, using the same design as was done on Pancam.

Dust Concentration

The local concentration of airborne dust would be measured by a pair of dust impact sensors. The atmospheric dust sensor (ADS) is a simplified version of the impact stage of the GIADA dust sensor, currently flying on Rosetta; another version flew on Beagle-2. It measures the momentum and rate of impact of airborne dust and sand with a piezoelectric sensing film, which generates a charge when grains impact onto it. This charge is amplified and captured by integral electronics. The sensor then produces an analog voltage output proportional to the grain momentum. This voltage is maintained until the sensor is reset via a logic line.

Two cylindrical dust sensors would be mounted on the mast, one near the bottom and the other near the top. Since the sensor measures particle momentum, simultaneous measurements of wind speed are useful in interpreting the sensor data in terms of particle mass and velocity. Each of the sensors has a mass of 15 gm, with a diameter of 20 mm and a height of 40 mm. The two sensors require <120 mW for continuous operation. The dust sensor is monitored at 4 kHz, and counts are accumulated for sampling periods ranging from 1–5 minutes. This would yield a data rate of 23 kbits/sol. Further details of the dust sensor instrument are provided in Table 3-8.

Table 3-8. Atmospheric Dust Sensors (Two)

Item	Value	Units
Type of instrument	Dust sensor	
Number of channels	4	
Size/dimensions (for each instrument)	0.04 height x 0.02 diameter	m x m
Instrument mass without contingency (CBE*)	0.015	kg
Instrument mass contingency	33%	%
Instrument mass with contingency (CBE+Reserve)	0.02	kg
Instrument average power without contingency	0.12	W
Instrument average power contingency	33%	%
Instrument average power with contingency	0.16	W
Instrument average science data rate [^] without contingency	0.0003	kbps
Instrument average science data [^] rate contingency	30%	%
Instrument average science data [^] rate with contingency	0.0003	kbps
Sensitivity	N/A	
Instrument fields of view (if appropriate)	N/A	degrees
Pointing requirements (knowledge)	N/A	degrees
Pointing requirements (control)	N/A	degrees
Pointing requirements (stability)	N/A	deg/sec

*CBE = Current best estimate

[^]Instrument data rate defined as science data rate prior to on-board processing

Flight System

The flight system for the MGN mission would consist of two identical, independent flight systems. Each flight system would include three flight elements: a lander, an entry system, and a cruise stage. The cruise stages would not have command and data handling (C&DH) or propulsion subsystems, rather the landers' C&DH and propulsion subsystems would be used during cruise and EDL. This architecture could minimize overall cost, mass, and power needs by focusing the complexity associated with the majority of the electronic systems of the entire flight system into a single flight element.

During launch, the flight systems would be stacked vertically with a dual payload adapter supporting the upper flight system, and the lower flight system attached directly to the Centaur upper stage of the launch vehicle. Shortly after launch, the upper stage would target Mars and complete the trans-Mars injection burn. This would be followed by the release of the first flight system from the top of the dual payload adapter. Once the first flight system is clear of the upper stage, the third and final Centaur upper stage burn would be initiated, which would provide the necessary delta-V to separate the flight systems entry time by approximately seven days. After the Centaur third burn, the dual payload adapter cover would be deployed and the second flight system released. By allowing the Centaur to perform this function, each flight system would avoid additional cost and mass increases due to use of a larger propellant tank to carry fuel needed to perform the separation burns themselves.

Launch would be scheduled for September 2022 with cruise durations of six months. During this time, several trajectory correction maneuvers (TCMs) would be used to maintain nominal trajectories. Approximately five minutes prior to entry, the entry system (with the lander inside) would separate from the cruise stage, which would proceed to burn up in the martian atmosphere. The entry system would initially use an aeroshell to decelerate during the hypersonic phase until it is safe to deploy the parachute. The entry system would further decelerate during the parachute phase. During this time, the heatshield, which would employ super lightweight ablator material to absorb the heat generated during entry, would be jettisoned.

After the heatshield has been jettisoned, the lander would be exposed for the first time to the martian atmosphere, giving the landing radar, which is mounted on the bottom of the lander deck, a view of the martian surface. The landing radar would then be able to collect altitude and velocity measurements, which would be used to determine the timing of the lander's separation from the backshell/parachute. The landing radar and IMU would provide the needed attitude, velocity, and altitude knowledge to allow for a safe landing velocity. This event would initiate the terminal descent phase of EDL, in which the lander would descend the final ~1,000 m to the surface using powered descent engines. The entire EDL sequence would be repeated seven days later with the second flight system.

Once the lander is safely on the surface of Mars, the solar arrays would be deployed and the checkout phase would begin. Shortly thereafter, the primary instrument (the seismometer) would be deployed to the surface using the robotic arm. Cameras mounted on the lander deck and robotic arm would provide images to help the mission operations team determine where the seismometer should be deployed.

Once the seismometer is deployed, the robotic arm would not need to be used again for the remainder of the mission, and there would be no further tactical operations. Each lander would then be operated as a simple monitoring station within routine operations. The mass of each flight element is provided in Table 3-9.

Table 3-9. Flight Element Masses

	Mass		
	CBE (kg)	% Cont.	MEV (kg)
Lander payload	13	42%	19
Lander bus	242	30%	314
Entry system	144	30%	187
Cruise stage	65	30%	84
Descent propellant	37	0%	37
Cruise propellant	29	0%	29

	Mass		
	CBE (kg)	% Cont.	MEV (kg)
Lander 1 “stack”	516	30%	670
Lander 2 “stack”	516	30%	670
Dual launch adapter	238	30%	310
Total launch mass	1,269	30%	1,650
Entry mass	428	30%	557
Landed mass	256	30%	333

Lander

The two identical MGN landers would be the primary flight elements for the mission. The landers would be designed to survive at least one martian year on the surface. Each lander would house a C&DH subsystem, which would not only operate during the primary science phase while on the surface, but also during the cruise and entry phases of the mission. This architecture, similar to what was used by the MPF, MER, and Phoenix missions, could minimize overall cost, mass, and power needs by focusing the complexity associated with the majority of the electronic systems of the entire flight system into a single flight element. Since data requirements for this mission are relatively low, the C&DH subsystem would contain just a 2 Gb non-volatile memory card.

The MGN mission would further benefit from this architectural approach by using a single propulsion subsystem for the cruise and EDL. By scarfing the TCM and reaction control system (RCS) thrusters through the backshell, the need for a second propulsion system on the cruise stage would be eliminated, saving significant mass and cost. Similarly, one of the two small deep space transponders (SDSTs) that would typically be required on each cruise stage (for redundancy) would instead be on the lander, where it could provide the hardware needed to conduct the radio science experiment and provide emergency X-band direct-to-Earth (DTE) communications. Operational data return would employ a UHF helix antenna and Electra-Lite radio, which would relay data twice a day to an existing relay asset. Both the C&DH and telecommunications subsystems are fully redundant.

The ACS hardware on the lander would include the IMU (which would be used during cruise and EDL) and the landing radar, which would be operational during the descent phase. The lander propulsion system would be a regulated monopropulsion hydrazine system using gaseous helium as a pressurant. There would be a total of 20 thrusters: 12 descent thrusters, 4 RCS, and 4 TCMs. The propulsion system would be fed through two propellant tanks and two pressurant tanks.

The primary structure of the lander would be made of aluminum and comprised of a lander deck supported by landing legs and struts. The lander would require three deployable legs. Other deployments include the solar arrays, IDA, and ATM mast.

Science requirements on landing site selection are minimal (~3,000 km lander separation and near the Tharsis region). Since exact landing location is not a driver for the science return, no guided entry or pinpoint landing is required, and 100 km by 20 km landing ellipses are acceptable. Safe landing ellipses can be examined and certified using Mars Reconnaissance Orbiter (MRO) High Resolution Imaging Science Experiment (HiRISE) images. This flexibility (from a science perspective) would allow landing site elevation and latitude to drive landing site selection. A power system with ultraflex solar arrays 4.2 m² in size and a 50 A-hr battery should enable landing site latitudes up to 20 North. The ability to minimize nighttime science data collection (SEIS only), and the tight thermal enclosure for the avionics (which minimizes needed heater power) allow the lander to survive worst-case martian winter nights. Lander mass and power, by subsystem, is provided in Table 3-10. Key lander characteristics are summarized in Table 3-11. Note that all average power values represent average power while active, during nominal surface operations, without any duty cycle reductions. Also, lander BOL and EOL energy generation values are shown in W-Hr/sol and assume 19.2 degrees north latitude, an arrival Ls of 47.9 deg, 40% maximum dust accumulation, with a dust tau of 1.0 during the dust season, and a dust tau of 0.5 during the remainder of the martian year.

Table 3-10. Lander Mass and Power

	Mass			Average Power		
	CBE (kg)	% Cont.	MEV (kg)	CBE (W)	% Cont.	MEV (W)
Structures and mechanisms	102	30%	133	0	43%	0
Thermal control	11	30%	15	14	43%	20
Propulsion (dry mass)	47	30%	61	0	43%	0
Attitude control	11	30%	14	0	43%	0
Command & data handling	11	30%	15	28	43%	40
Telecommunications	11	30%	14	49	43%	70
Power	48	30%	63	17	43%	25
Total Flight Element Dry Bus	242	30%	314	108	43%	155

Table 3-11. Lander Characteristics

Flight System Element Parameters (as appropriate)	Value/ Summary, units
General	
Design life, months	30
Structure	
Structures material (aluminum, exotic, composite, etc.)	Aluminum/composites
Number of articulated structures	1 robotic arm
Number of deployed structures	3 lander legs, 2 solar panels, 1 instrument deployment arm, 1 ATM mast
Aeroshell diameter, m	N/A
Thermal Control	
Type of thermal control used	Passive radiators, heaters, heat pipes
Propulsion	
Estimated delta-V budget, m/s	Descent: 241 m/s Cruise (TCM+ACS) : 55 m/s
Propulsion type(s) and associated propellant(s)/oxidizer(s)	Type: regulated monoprop Propellant: hydrazine Pressurant: helium
Number of thrusters and tanks	12 x 72 lbf descent thrusters, 4 x 5 lbf TCM thrusters, 4 x 1 lbf RCS thrusters, 2 propellant tanks, 2 pressurant tanks
Specific impulse of each propulsion mode, seconds	Descent: 227 s Entry RCS: 100–215 s Cruise TCMs: 100–215 s
Attitude Control	
Control method (3-axis, spinner, grav-gradient, etc.)	3-axis
Control reference (solar, inertial, Earth-nadir, Earth-limb, etc.)	Landing radar, IMU
Attitude control capability, degrees	During entry/descent: 5 deg
Attitude knowledge limit, degrees	During entry/descent: 0.5 deg

Flight System Element Parameters (as appropriate)	Value/ Summary, units
Agility requirements (maneuvers, scanning, etc.)	N/A
Articulation/#-axes (solar arrays, antennas, gimbals, etc.)	4 DOF robotic arm
Sensor and actuator information (precision/errors, torque, momentum storage capabilities, etc.)	<1 cm knowledge of robotic arm end effector
Command & Data Handling	
Flight Element housekeeping data rate, kbps	2 kbps
Data storage capacity	2 Gb NVM
Maximum storage record rate, Mbps	20
Maximum storage playback rate, Mbps	20
Power	
Type of array structure (rigid, flexible, body mounted, deployed, articulated)	Deployed UltraFlex
Array size, meters x meters	4.2 m ²
Solar cell type (Si, GaAs, multi-junction GaAs, concentrators)	UTJ
Expected energy generation per martian sol at beginning of life (BOL) and end of life (EOL), Watt-Hr/sol	3741 (BOL), 1881 (EOL)
Average energy consumption, Watt-Hr/sol	900
Battery type (NiCd, NiH, Li-ion)	Li-ion
Battery storage capacity, amp-hours	50 A-Hr

Entry System

The MGN entry system design for two identical landers is based on the Phoenix 2007 design. The entry vehicle would separate from the cruise stage and rely on the RCS thrusters for the attitude alignment approximately five minutes prior to entry point. The MGN entry system could potentially utilize the 3-axis control capability during entry; however, similar to the Phoenix-flown architecture, MGN would enter the martian atmosphere ballistically with no active control. The mechanical design of the vehicle consists of an aeroshell that would protect the lander during cruise and hypersonic entry phase, and a supersonic parachute to slow the entry vehicle to a required velocity/altitude prior to the powered terminal descent of the MGN lander. The aeroshell mechanical design is composed of a heatshield and backshell, which are protected by a thermal protection system (TPS) such as SLA-561. The TPS mass would be slightly increased due to the higher entry speed in comparison to Phoenix. The 2022 mission would use the same aeroshell diameter (2.65 m) as was used on the MPF, MER, and Phoenix flight projects. The heatshield geometry would rely on the Viking shape. Also similar to MPF, MER and Phoenix, the supersonic parachute would be disk-gap-band, which would preserve the Viking chute design. The IMU and descent sensor (for altitude) would be used to trigger the parachute opening and lander powered descent. Both units would be carried by the lander.

The only other hardware present on the entry system would be a UHF antenna for EDL communications to an orbiting asset. Power, propulsion, C&DH, ACS, and telecommunication functions during entry would be performed by lander subsystems. Entry system mass and power, by subsystem, is provided in Table 3-12. Key entry system characteristics are summarized in Table 3-13.

Table 3-12. Entry System Mass and Power

	Mass			Average Power		
	CBE (kg)	% Cont.	MEV (kg)	CBE (W)	% Cont.	MEV (W)
Structures and mechanisms	135	30%	175	0	43%	0
Thermal control	5	30%	6	45	43%	64
Propulsion (dry mass)	0	0%	0	455	43%	651
Attitude control	0	0%	0	60	43%	86
Command & data handling	0	0%	0	28	43%	40
Telecommunications	4	30%	6	49	43%	70
Power	0	0%	0	156	43%	223
Total Flight Element Dry Bus	144	30%	187	793	43%	1134

Table 3-13. Entry System Characteristics

Flight System Element Parameters (as appropriate)	Value/ Summary, units
General	
Design life, months	6 months
Structure	
Structures material (aluminum, exotic, composite, etc.)	Aluminum, SLA-561
Number of articulated structures	N/A
Number of deployed structures	1 heatshield, 1 backshell, 1-DGB parachute
Aeroshell diameter, m	2.65 m
Thermal Control	
Type of thermal control used (TPS)	SLA-561V and SLA-561S
Propulsion	Function performed by lander
Estimated delta-V budget, m/s	N/A
Propulsion type(s) and associated propellant(s)/oxidizer(s)	N/A
Number of thrusters and tanks	N/A
Specific impulse of each propulsion mode, seconds	N/A
Attitude Control	Function performed by lander
Control method (3-axis, spinner, grav-gradient, etc.)	N/A
Control reference (solar, inertial, Earth-nadir, Earth-limb, etc.)	N/A
Attitude control capability, degrees	N/A
Attitude knowledge limit, degrees	N/A
Agility requirements (maneuvers, scanning, etc.)	N/A
Articulation/#-axes (solar arrays, antennas, gimbals, etc.)	N/A
Sensor and actuator information (precision/errors, torque, momentum storage capabilities, etc.)	N/A
Command & Data Handling	Function performed by lander
Flight Element housekeeping data rate, kbps	N/A
Data storage capacity, Mbits	N/A
Maximum storage record rate, kbps	N/A
Maximum storage playback rate, kbps	N/A

Flight System Element Parameters (as appropriate)	Value/ Summary, units
Power	Function performed by lander
Type of array structure (rigid, flexible, body mounted, deployed, articulated)	N/A
Array size, meters x meters	N/A
Solar cell type (Si, GaAs, multi-junction GaAs, concentrators)	N/A
Expected power generation at beginning of life (BOL) and end of life (EOL), watts	N/A
On-orbit average power consumption, watts	N/A
Battery type (NiCd, NiH, Li-ion)	N/A
Battery storage capacity, amp-hours	N/A

Cruise Stage

The cruise stage would be made up of a simple circular primary structure, solar arrays to provide power to the lander electronics, an X-band telecommunications system, sun sensor and star tracker for attitude determination, and a thermal control subsystem. All other functions (C&DH and propulsion) are performed by the lander hardware. The TCM and RCS thrusters are scarfed through the entry system's backshell to allow the lander's propulsion system to also be used during the cruise phase.

The cruise stage structure would essentially be a launch adapter ring with necessary cruise hardware attached. The solar array mechanisms would be the only significant mechanisms on the cruise stage. The cruise stage power subsystem would consist of approximately 3–4 m² deployed solar panels that support the cruise stage telecommunications, attitude control, and thermal subsystems along with the lander electronics and propulsion subsystems. The solar arrays would support operation of the spacecraft until approximately five minutes prior to entry. The cruise stage would have no power electronics on board. The cruise stage telecommunications subsystem would be solely X-band and contain a low-gain patch antenna, fixed medium-gain antenna, and SDST as the primary components. The attitude control subsystem on the cruise stage would perform attitude determination by the use of sun sensors, star trackers, and the lander's IMU. The control portion of the attitude control subsystem would be the lander RCS and TCM thrusters. Lastly, the thermal control subsystem on the cruise stage would consist of a minimal number of heat pipes, heaters, thermostats, multilayer insulation (MLI), and surface coatings.

As discussed, there would be only five subsystems on the cruise stage and no instruments. Table 3-14 shows a breakdown of the subsystems. Thirty percent contingency would be carried on all subsystems and the maximum expected value of the cruise stage would be approximately 85 kg. Cruise stage mass and power, by subsystem, are provided in Table 3-14. Key cruise stage characteristics are summarized in Table 3-15.

Table 3-14. Cruise Stage Mass and Power

	Mass			Average Power		
	CBE (kg)	% Cont.	MEV (kg)	CBE (W)	% Cont.	MEV (W)
Structures and mechanisms	32	30	41	0	43%	0
Thermal control	3	30	3	4	43%	6
Propulsion (dry mass)	0	30	0	47	43%	67
Attitude control	5	30	7	51	43%	73
Command & data handling	0	30	0	28	43%	40
Telecommunications	8	30	10	49	43%	70
Power	18	30	23	13	43%	19
Total Flight Element Dry Bus	66	30	84	192	43%	275

Table 3-15. Cruise Stage Characteristics

Flight System Element Parameters (as appropriate)	Value/ Summary, units
General	
Design life, months	6 months
Structure	
Structures material (aluminum, exotic, composite, etc.)	Aluminum
Number of articulated structures	N/A
Number of deployed structures	2 solar panels
Aeroshell diameter, m	N/A
Thermal Control	
Type of thermal control used	Passive
Propulsion	Function performed by lander
Estimated delta-V budget, m/s	N/A
Propulsion type(s) and associated propellant(s)/oxidizer(s)	N/A
Number of thrusters and tanks	N/A
Specific impulse of each propulsion mode, seconds	N/A
Attitude Control	
Control method (3-axis, spinner, grav-gradient, etc.)	3-axis
Control reference (solar, inertial, Earth-nadir, Earth-limb, etc.)	Inertial, solar
Attitude control capability, degrees	0.1 deg
Attitude knowledge limit, degrees	0.3 deg
Agility requirements (maneuvers, scanning, etc.)	N/A
Articulation/#-axes (solar arrays, antennas, gimbals, etc.)	N/A
Sensor and actuator information (precision/errors, torque, momentum storage capabilities, etc.)	N/A
Command & Data Handling	Function performed by lander
Flight Element housekeeping data rate, kbps	N/A
Data storage capacity, Mbits	N/A
Maximum storage record rate, kbps	N/A
Maximum storage playback rate, kbps	N/A

Flight System Element Parameters (as appropriate)	Value/ Summary, units
Power	
Type of array structure (rigid, flexible, body mounted, deployed, articulated)	Rigid
Array size, meters x meters	3.5 m ²
Solar cell type (Si, GaAs, multi-junction GaAs, concentrators)	UTJ
Expected power generation at beginning of life (BOL) and end of life (EOL), watts	1201 (BOL), 407 (EOL)
On-orbit average power consumption, watts	182
Battery type (NiCd, NiH, Li-ion)	NA
Battery storage capacity, amp-hours	NA

Stacked Configuration Adapter

Since this is a two-lander mission, there is a requirement to launch two spacecraft on one launch vehicle. As discussed in the Key Trades section, the best method to meet this requirement would be to employ a stacked configuration as illustrated in Figure 2-2. This configuration would allow one spacecraft (the lower one) to be attached directly to the launch vehicle. The other spacecraft (the upper one) would be attached to a reach-around adapter and would sit directly above the lower one. The deployment sequence would jettison the upper vehicle first then would jettison the upper half of the dual adapter. This would expose the lower spacecraft to space and would allow it to be released. The adapter for this configuration would have a maximum expected value (MEV) of 310 kg.

Concept of Operations and Mission Design

Two identical Phoenix-class spacecraft would be launched in a stacked vertical configuration on a single Atlas V 401 launch vehicle. The launch would take place at the Cape Canaveral Air Force Station on September 7, 2022 with an allocated 21-day launch period ending on September 26, 2022. Each day would include one launch opportunity with subsequent opportunities following the next day. More detailed trajectory data on each Earth-Mars opportunity within this launch window can be found in Table 3-16. The mission design for this particular Mars arrival opportunity was driven by the relatively short cruise phase and minimum entry speed for Mars EDL conditions.

The Atlas V 401 would place the flight system into a low Earth orbit with an altitude of 185–195 km. The ground stations provide sufficient tracking while the two spacecraft continue coast phase as a single flight unit to a location where the interplanetary orbit injection is planned to occur. At the targeted injected state (launch +55 min), the Centaur upper stage would perform a trajectory injection maneuver (second burn), which would send the first spacecraft toward Mars. The upper spacecraft (cruise stage, entry system, and lander) would separate, while the other spacecraft would remain attached to the Centaur with the adapter. The proposed mission logistics suggest a seven-day separation between the two EDL sequences. Hence, to provide the proper separation between the spacecraft arrivals, the Centaur would utilize a third burn to perform a small plane change maneuver ($\Delta V \sim 90$ m/s), which would delay the Mars arrival epoch for the second spacecraft by seven days. Once the second spacecraft is separated and sent on the way to Mars, the launch vehicle would bias away from Mars in agreement with planetary protection protocols. At launch +15 days and Launch +10 days, both spacecraft would finish the system checkup and execute the first TCM (TCM-1). This maneuver would have two purposes: to remove the launch bias and to clean up the launch dispersions. The ΔV budget of each spacecraft would allow performance of 5–6 more TCMs prior to Mars entry.

Both spacecraft would follow a direct, Type I transfer to Mars with a total flight time of 194 days to 213 days. The worst-case launch C3 in the present Earth-Mars launch window is 23.722 km²/sec² and the worst case DLA is 49.33 degrees. Mars entry velocity does not change significantly across the 21 launch day period with a maximum of 5.996 km/s. This value is slightly higher in comparison to the Phoenix 2008 $V_{\text{entry}}=5.6$ km/s, but would be within the design capabilities of the 2022 EDL system design.

Table 3-16. Earth-Mars 2022 Type I Trajectory with Launch Window

Day	LD	AD	TOF (day)	C3 (km ² /sec ²)	DLA (deg)	RLA (deg)	VHP (km/sec)	DAP (deg)	RAP (deg)	VENTRY (km/sec)	Ls (deg)	SEP (deg)
1	220907	230408	213	18.641	49.333	57.02	3.41	-23.351	46.246	5.99617	47.914	78.849
2	220908	230408	212	18.57	48.419	56.358	3.404	-22.795	46.686	5.99276	47.914	78.849
3	220909	230408	211	18.54	47.523	55.697	3.399	-22.259	47.094	5.98993	47.914	78.849
4	220910	230408	210	18.549	46.646	55.039	3.395	-21.742	47.472	5.98766	47.914	78.849
5	220911	230408	209	18.595	45.786	54.387	3.392	-21.243	47.822	5.98596	47.914	78.849
6	220912	230408	208	18.679	44.942	53.744	3.389	-20.759	48.144	5.98426	47.914	78.849
7	220913	230408	207	18.799	44.115	53.112	3.387	-20.29	48.44	5.98312	47.914	78.849
8	220914	230408	206	18.956	43.304	52.492	3.386	-19.833	48.712	5.98256	47.914	78.849
9	220915	230408	205	19.149	42.508	51.886	3.385	-19.389	48.959	5.98199	47.914	78.849
10	220916	230408	204	19.378	41.73	51.297	3.384	-18.955	49.183	5.98143	47.914	78.849
11	220917	230408	203	19.643	40.967	50.725	3.384	-18.531	49.384	5.98143	47.914	78.849
12	220918	230408	202	19.945	40.221	50.172	3.385	-18.116	49.563	5.98199	47.914	78.849
13	220919	230408	201	20.283	39.492	49.639	3.385	-17.708	49.721	5.98199	47.914	78.849
14	220920	230408	200	20.659	38.78	49.127	3.386	-17.308	49.858	5.98256	47.914	78.849
15	220921	230408	199	21.072	38.086	48.637	3.388	-16.914	49.975	5.98369	47.914	78.849
16	220922	230408	198	21.523	37.409	48.169	3.389	-16.525	50.073	5.98426	47.914	78.849
17	220923	230408	197	22.013	36.75	47.725	3.391	-16.14	50.15	5.98539	47.914	78.849
18	220924	230408	196	22.542	36.11	47.304	3.393	-15.76	50.209	5.98652	47.914	78.849
19	220925	230408	195	23.112	35.489	46.907	3.395	-15.383	50.248	5.98766	47.914	78.849
20	220926	230408	194	23.722	34.886	46.534	3.398	-15.009	50.27	5.98936	47.914	78.849
				23.722						5.99617		

The data tracking and communications between Earth and the two spacecraft during the cruise phase would be supported by the traditional set of DSN stations located in Canberra, Goldstone, and Madrid. Tracking would include Doppler, ranging, and Δ DOR measurements. The data tracking for navigation would require two passes per week for each spacecraft during the cruise phase with increased tracking frequency at Mars entry minus 30 days for each of the EDLs. The tracking would normally rely on the 34 m antennas with some occasional use of 70 m antennas for EDL critical event coverage.

The Mars 2022 landing opportunity would be favorable from the EDL standpoint. The entry velocity would not be excessively high and both landers would arrive at $L_s = 47.9$ degrees, which constitutes a martian spring (northern latitudes) and avoids any global dust storm seasons. A Phoenix-like EDL sequence is presented in Figure 3-7. Two preliminary landing locations within the Chryse area have been suggested for the MGN mission. The exact coordinates are recorded in Table 3-17. Both potential landing targets satisfy a predicted dispersion ellipse ($180 \text{ km} \times 30 \text{ km}$) from the ballistic entry, rock abundance, and MOLA surface slope considerations constrained by the Phoenix-type legged lander design. These landing sites at -3.3 km and -2 km MOLA elevation would satisfy the science requirements and could provide an adequate timeline margin from the altitude standpoint. A more detailed representation of the proposed landing sites is illustrated in Figure 3-8.

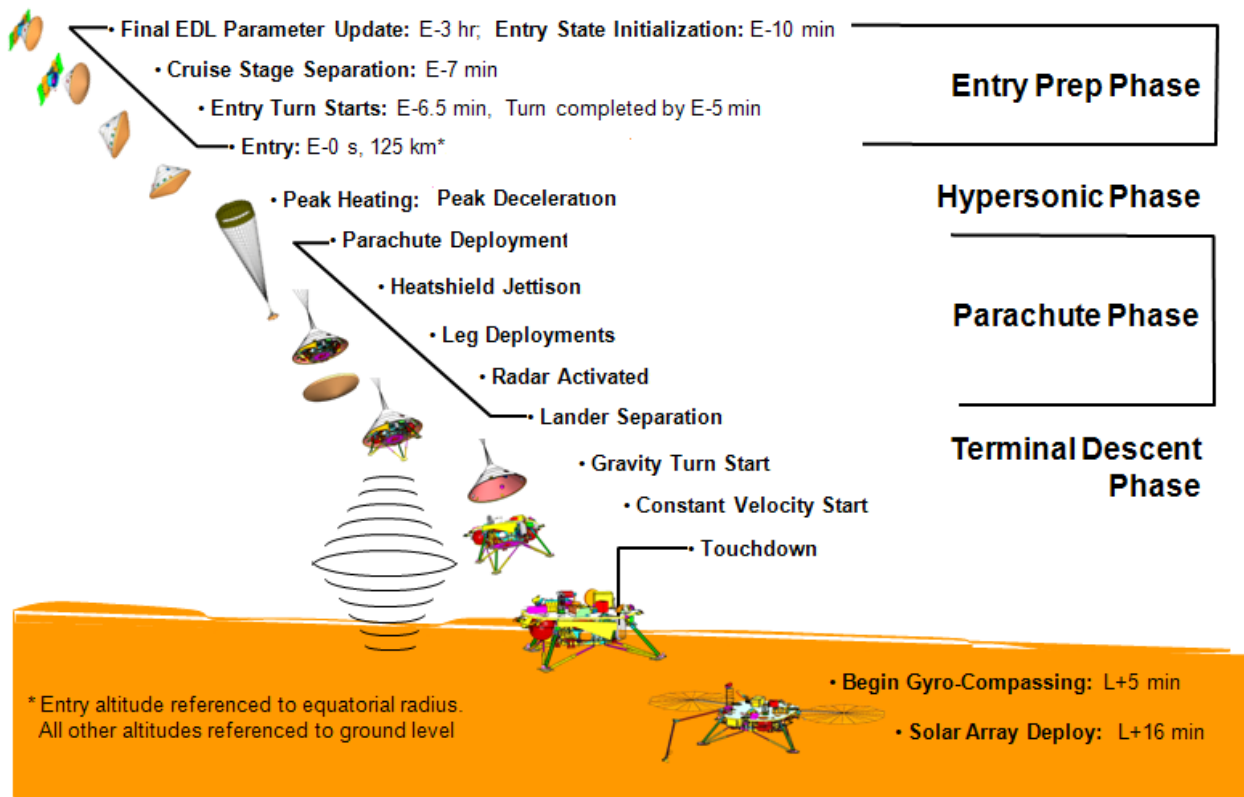


Figure 3-7. EDL Sequence (Legged Lander)

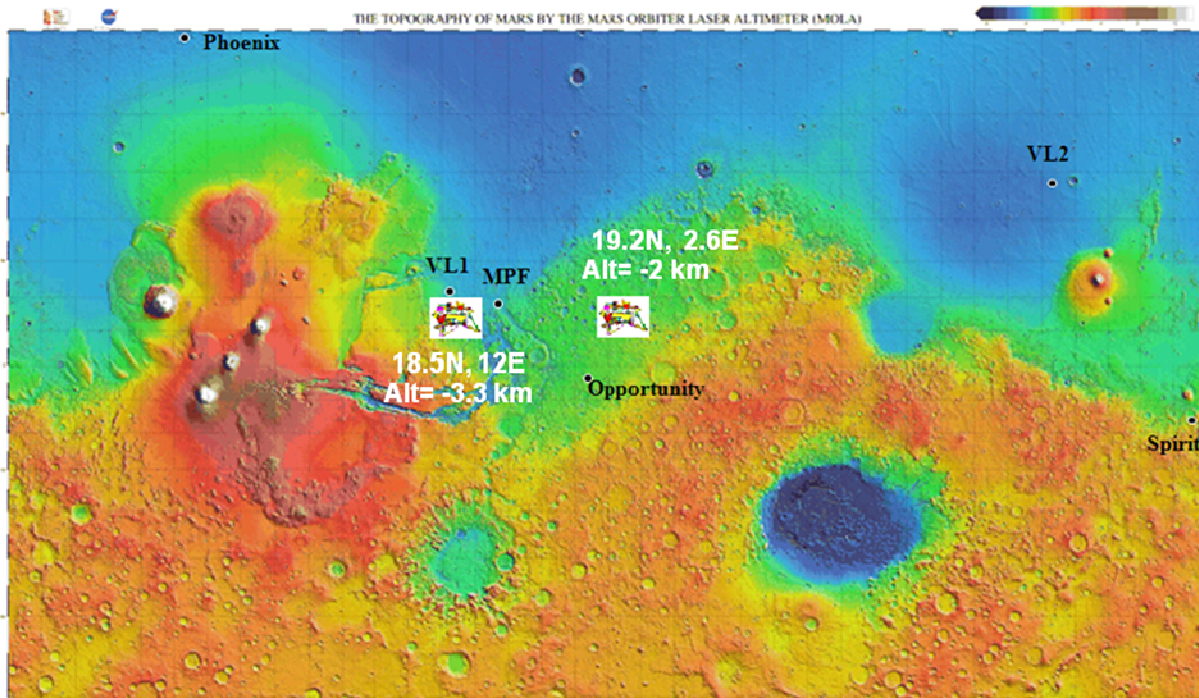


Figure 3-8. Mars Landing Sites

Table 3-17. Mission Design

Parameter	Value	Units
Orbit parameters (apogee, perigee, inclination, etc.)	N/A	
Landing target lander I	Lat 18.5N Lon 12E	Deg
Landing target lander II	Lat 19.2 Lon 2.6E	Deg
Mission lifetime	30	Mos
Maximum eclipse period	NA	Min
Launch site	Cape Canaveral	
Total spacecraft #1 mass with contingency (includes instruments and propellant)	670	Kg
Total spacecraft #2 mass with contingency (includes instruments)	670	Kg
Propellant mass without contingency (both spacecraft)	132	Kg
Propellant contingency	0	%
Propellant mass with contingency (both spacecraft)	132	Kg
Launch adapter mass with contingency	310	Kg
Total launch mass	1,650	Kg
Launch vehicle	Atlas V 401	Type
Launch vehicle lift capability	2,058	Kg
Launch vehicle mass margin	408	Kg
Launch vehicle mass margin (%)	20%	%

Two MGN landers would be launched on the same launch vehicle and separate shortly after launch. Each lander would travel to Mars on its own cruise stage, scheduled to arrive with roughly one week separation. The first lander would undergo full deployment before the second lander arrives.

All tracking and communications between Earth and the spacecraft during the cruise phase would be performed with the DSN. Tracking would include Doppler and Δ DOR measurement types. The cruise phase tracking would average one pass per week for each spacecraft, with increased tracking for the approach and EDL phases. The tracking would use 34 m stations with the exception of the 8 hours around EDL that would utilize a 70 m station equivalent for the critical event.

Once on the surface of Mars, all communication with the lander would be performed with a UHF link to an available relay orbiter. The orbiter would have a DTE link with the DSN. During checkout and the early characterization phase, there would be daily relay links. After one month, this would be reduced to a weekly relay link. In addition to the relay communications link, there would be a weekly one-hour radio science X-band two-way Doppler/ranging link between the DSN and alternate lander (one lander each week). This link would support a carrier-only signal and could not be used for commanding or data return.

All data associated with instrument operations would be relayed to Earth via an orbiter. It is expected that the landers would transmit approximately 280 Mbits using one pass per week to a relay orbiter using the UHF link. The DSN would transmit weekly and monthly commands to the relay orbiter via X-band for retransmission to the lander across the UHF link. The data would be at least 95% complete with latency no longer than 28 sols. The operations would be a mission-specific implementation of the JPL mission operations and ground systems as used previously for Phoenix and other Mars missions. Standard JPL operations processes and procedures would be used.

The operations support would include double shifts for the first 60 days, then would change to single prime shift operations with a single team supporting both landers for the remainder of the surface science operations. The mission operations would include processing to Level 0 data and maintenance for the life of the mission. Further processing and archiving would be the responsibility of the science operations. The operations are assumed to be conducted at JPL. Relevant parameters of the mission operations and ground data systems are provided in Table 3-18. All DSN tracks and tracking phases are shown in Table 3-19.

Table 3-18. Mission Operations and Ground Data Systems

Downlink Information	Cruise	Approach, EDL, and Checkout	Surface Ops
Number of contacts per week	2	14	2
Number of weeks for mission phase, weeks	18	10	103
Downlink frequency band, GHz	X-band	X-band & UHF relay	UHF relay
Telemetry data rate(s), kbps	1	8	32–2,048
Transmitting antenna type(s) and gain(s), DBi	MGA	UHF wrap-around	Helix
Transmitter peak power, Watts	70	70	70
Downlink receiving antenna gain, DBi	34 m BWG antenna gains vary		
Transmitting power amplifier output, Watts	17	8.5	8.5
Total daily data volume, (MB/day)	N/A	N/A	70
Uplink Information			
Number of uplinks per day	1/week	Daily	1/week
Uplink frequency band, GHz	X-band	X-band & UHF relay	UHF relay
Telecommand data rate, kbps	2	2	2
Receiving antenna type(s) and gain(s), DBi	X-band MGA/LGA	X-band MGA/LGA	UHF

Table 3-19. DSN Tracking Schedule

Support Period		Antenna Size (m)	Service Year	Hours per Track	No. Tracks per Week	No. Weeks Required
No.	Name (description)					
1	Launch and operations	34 BWG	2016	8	21.0	2.0
2	Launch and operations	34 BWG	2016	8	14.0	2.0
3	Cruise	34 BWG	2016	8	2.0	18.0
3	DDOR	34 BWG	2016	1	2.0	18.0
4	Landing preparation—approach	34 BWG	2016	8	14.0	4.0
4	DDOR	34 BWG	2016	1	21.0	4.0
5	Landing	34 BWG	2016	8	14.0	2.0
5	DDOR	34 BWG	2016	8	14.0	2.0
5	EDL	70	2016	8	1.0	2.0
6	Relay	34 BWG	2016	0.2	7.0	4.0
7	Relay	34 BWG	2016	0.1	1.0	103.0
7	Radio science	34 BWG	2016	1	1.0	103.0

Planetary Protection

In accordance with NPR 8020.12C, the MGN mission is expected to be a Planetary Protection Category IV a mission. Accordingly, the MGN project would demonstrate that its mission meets the Category IV planetary protection requirements per NPR 8020.12C, Appendix A.2. The planetary protection category of the mission would be formally established by the NASA Planetary Protection Officer (PPO) in response to a written request from the MGN Project Manager, submitted by the end of Phase A.

The MGN mission plans to assemble the spacecraft hardware in Class 8 cleanroom facilities with appropriate controls. The bioburden requirements would be met by using a combination of cleaning and dry heat microbial reduction (DHMR). Cleaning would be done by either alcohol wipe or precision cleaning compatible hardware. DHMR would be used for portions of the spacecraft having large surface areas (e.g., MLI, parachute), surfaces that are difficult to clean (e.g., honeycomb structures, batting insulation), and portions of the spacecraft having large accountable encapsulated non-metallic volumes (e.g., thermal protection system of the aeroshell). Credit would be taken for high-temperature cures and manufacturing processes whenever possible. The MGN mission would perform bioassay sampling of the spacecraft hardware at last access to determine the level of bioburden present on the spacecraft at launch and to determine the diversity of the microbial population. There would also be bioassays performed at intermediate steps to monitor the spacecraft during assembly and test activities. MGN personnel would perform the sampling as directed by the NASA PPO office for the PPO's independent verification bioassays. An entry heating analysis would be performed, similar to the analysis performed for past Mars missions (up to and including Mars Science Laboratory), to determine which outboard surfaces of the aeroshell's heatshield and backshell would be sterilized by heating to greater than 500C during Mars entry. If entry heating is found to be insufficient to sterilize the entire outboard surface of the aeroshell, then additional measures would be taken to protect the aeroshell and lander from recontamination by the cruise stage and launch vehicle during launch decompression. An entry heating and break-up analysis, similar to the analysis performed by the Phoenix project, would be performed to demonstrate that the cruise stage would be sterilized by heating to greater than 500°C during Mars entry. If MGN is unable to demonstrate adequate heating, then the cruise stage would undergo cleaning and DHMR processes as needed to meet the bioburden requirements. The entry heating and breakup analysis would be reported in the pre-launch planetary protection report. The organic materials list would be compiled and the required samples collected for archival. The organic materials list would also be reported in the pre-launch planetary protection report. The organic materials samples would be archived at JPL by the Biotechnology and Planetary Protection Group. The non-impact requirements would be demonstrated by analyses performed by the navigation team at JPL, similar to the analyses performed in the past by the MPF, MPL, and MER projects. The navigation team at JPL would also identify the location

of the landing point on Mars. That location would be reported in the planetary protection end-of-mission report.

Risk List

This mission concept study identified two moderate and seven low risks as significant at the system level. This is not an exhaustive list; only significant risks are listed. For example, there would be a small likelihood that both spacecraft might not separate, leading to the loss of the mission. However, the probability of this risk is so low that it is not listed. The mission is designed to be relatively low cost and low risk for a mission with two in-situ landers, maximizing the use of known approaches, architectures, and flight elements. However, no specific hardware or software reuse is assumed. Both moderate risks would be operations risks related to EDL. Due to the early stage of the design and the limited study time, no risk mitigations were identified. All of these risks are common for any in-situ vehicle on Mars.

Figure 3-9 provides a 5 × 5 risk chart that shows the distribution of the identified risks. Table 3-20 provides a high-level summary with specific descriptions of each risk as assessed by subsystem engineers. Table 3-21 provides the risk level definitions for both mission and implementation risks.

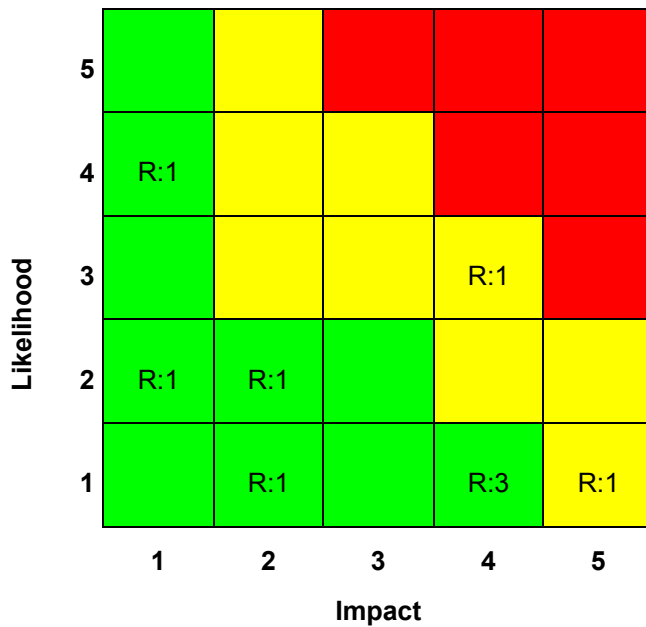


Figure 3-9. Risk Chart

Table 3-20. Detailed Risk Description and Mitigation Strategy

Risk	Level	Description	Impact	Likelihood	Mitigation
EDL failure of single spacecraft (mission risk)	M	EDL, by definition, is a complex set of events. EDL is single string; therefore, an anomaly during any phase of EDL may result in loss of lander.	4	3	Mission implements proven EDL strategy and uses two landers.
EDL failure of two spacecraft (mission risk)	M	Failure of both landers is low but would lead to total loss of mission.	5	1	Mission implements proven EDL strategy.
Solar array dust accumulation (implementation risk)	L	Power will be diminished during surface operations due to dust accumulation on the solar panels. Power levels may become too low to operate instruments.	2	2	Mitigation includes an oversized solar array. Another possible mitigation is development of a dust removal system.
Spacecraft separation failure (operations risk)	L	The mission plans for two spacecraft. If one spacecraft is lost, then 75% of science would be lost.	4	1	Design includes redundant separation mechanisms.
Robotic arm failure on one lander (operations risk)	L	If the arm fails to deploy, the seismometer would lose all primary science.	4	1	Design implements JPL's Design Principles.
Relay asset risk (operations risk)	L	Mission design requires that data from the landers be relayed to an existing Mars orbiter. There is some uncertainty regarding the existence of this orbiter and how the relay telecommunications would be configured.	4	1	No mitigation was identified during study.
Planetary protection requirements for EDL might become much more stringent (implementation risk)	L	The NASA PPO could impose a 99% reliability requirement on the EDL systems of Mars landers. In the event that a spacecraft cannot meet the reliability requirement, the spacecraft must meet a total (surface, mated, and encapsulated) bioburden limit. Meeting the biological cleanliness requirement would require increased use of microbial reduction techniques (i.e., dry heat microbial reduction).	1	4	No mitigation was identified during study.
Failure to land as required (operations risk)	L	The vehicle might land on rocks, at an overly steep angle, or on ground that is not level. This could cause a partial loss of science.	2	1	Landing sites have been extensively studied based on years of martian observation. The MGN landing sites would require certification prior to selection.

Risk	Level	Description	Impact		Mitigation
			Impact	Likelihood	
Planetary protection requirements not fully costed (implementation risk)	L	Hardware subsystems might not have adequately captured the cost of meeting planetary protection requirements.	1	2	No mitigation was identified during study.

Table 3-21. Risk Level Definitions

Levels	Mission Risk		Implementation Risk	
	Impact	Likelihood of Occurrence	Impact	Likelihood of Occurrence
5	Mission failure	Very high, >25%	Consequence or occurrence is not repairable without engineering (would require >100% of margin)	Very high, ~70%
4	Significant reduction in mission return (~25% of mission return still available)	High, ~25%	All engineering resources would be consumed (100% of margin consumed)	High, ~50%
3	Moderate reduction in mission return (~50% of mission return still available)	Moderate, ~10%	Significant consumption of engineering resources (~50% of margin consumed)	Moderate, ~30%
2	Small reduction in mission return (~80% of mission return still available)	Low, ~5%	Small consumption of engineering resources (~10% of margin consumed)	Low, ~10%
1	Minimal (or no) impact to mission (~95% of mission return still available)	Very low, ~1%	Minimal consumption of engineering resources (~1% of margin consumed)	Very low, ~1%

4. Development Schedule and Schedule Constraints

High-Level Mission Schedule

A feasible schedule for the MGN mission is provided as Figure 4-1. The mission complexity is consistent with other New Frontiers–class missions and, thus, the standard JPL reference schedule for announcement of opportunity (AO) driven missions. The reference schedules used are derived from the JPL mission schedule database, which extends back to the Voyager mission.

Phoenix is the closest analogy to this mission. Though the MGN mission would have fewer instruments and thus a much simpler and lighter payload, there would be two independent flight systems. Therefore, the development duration for MGN would be somewhat longer than the Phoenix mission. All elements (i.e., cruise stage, entry stage, and lander) would have the same basic schedule as displayed in Figure 4-1.

No major schedule drivers or long-lead items need to be addressed. Table 4-1 provides the duration for all key phases. As MGN would be proposed as a New Frontiers–competed mission, all instruments and flight elements would be delivered at the beginning of system-level I&T.

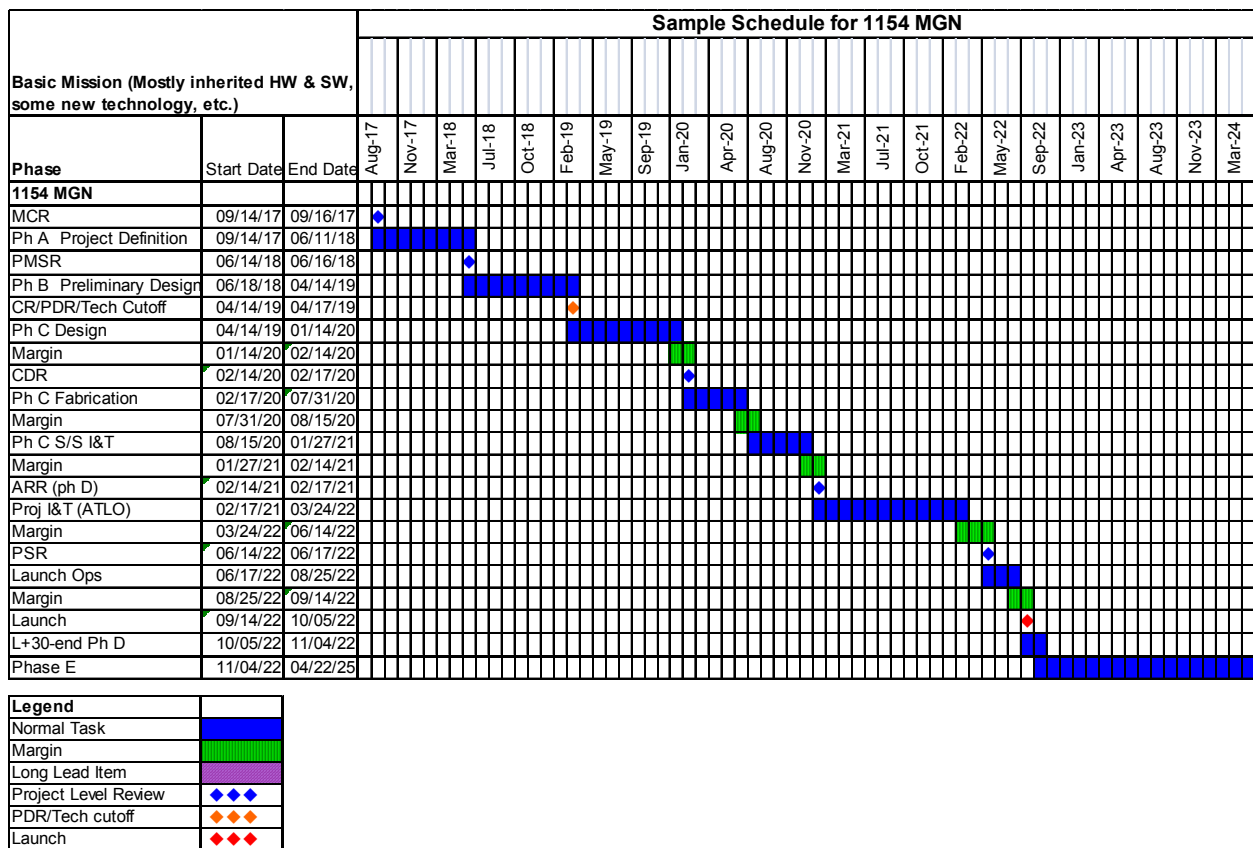


Figure 4-1. Mission Schedule

Table 4-1. Key Phase Duration

Project Phase	Duration (Months)
Phase A – Conceptual design	9
Phase B – Preliminary design	10
Phase C – Detailed design	22
Phase D – Integration & test	20
Phase E – Primary mission operations	30
Phase F – Extended mission operations	4
Start of Phase B to PDR	10
Start of Phase B to CDR	20
System-level integration & test	16
Project total funded schedule reserve	5.5
Total development time Phase B–D	52

Technology Development Plan

No technology development would be required for the baseline mission. Therefore, no technology development plan is provided here.

Development Schedule and Constraints

No particular schedule constraints exist for this mission other than those that apply to all Mars missions.

As with any Mars mission, a 21-day launch opportunity for this trajectory type occurs approximately every two years. The MGN mission would be scheduled to launch in September 2022. If a schedule slip should occur, it would be possible to launch in 2024 or launch using a Type III/IV trajectory. A slip to 2024 would be a cost upper to continue work, mothball the flight system, retain a skeletal team, re-train a flight team, and re-test the flight system. A Type III/IV trajectory would result in a significantly longer cruise duration (up to 30 months), which would most likely result in a substantial cost impact. Further evaluation is needed to quantify the cost impact of either launch-slip option.

ATLO Flow for Two Landers

I&T for the first lander would take 14 months. The second lander would not require the same extensive flight qualification testing of the first; therefore, I&T is expected to take 10 months. Start of I&T for the second lander would be staggered by six months. There would be a schedule savings if the start of I&T for the first and second units can be shifted as close as 1–4 months. This schedule savings might result in a cost savings. The trade of having a larger I&T workforce versus a longer period of I&T should be considered.

5. Mission Life-Cycle Cost

Costing Methodology and Basis of Estimate

JPL's Advanced Project Design Team (Team X) generates a most likely cost for the JPL standard work breakdown structure (WBS) that may be tailored to meet the specific needs of the mission being evaluated. These estimates are done at WBS levels 2 and 3 and are based on various cost estimating techniques. These methods are not exclusive to each other and are often combined. The various estimating techniques consist of grassroots techniques, parametric models, and analogies. The models for each station at Team X have been built (total of about 33) and validated, and they are each owned by the responsible line organization. The models are under configuration management control and are utilized in an integrated and concurrent environment, so the design and cost parameters are linked. These models are customized and calibrated using actual experience from completed JPL planetary missions. In applying these models it has been found that the resultant total estimated Team X mission costs have been consistent with mission actual costs.

The cost estimation process begins with the customer providing the base information for the cost estimating models and defining the mission characteristics, such as:

- Mission architecture
- Payload description
- Master equipment list (MEL) with heritage assumptions
- Functional block diagrams
- Spacecraft/payload resources (mass [kg], power [W])
- Phase A–F schedule
- Programmatic requirements
- Model specific inputs

Most of the above inputs are provided by the customer through a Technical Data Package. For Decadal Survey missions, the following specific guidelines were also followed:

- Reserves were set at 50% for Phases A–D.
- Reserves were set at 25% for Phase E.
- The launch vehicle cost was specified in the ground rules.

Cost Estimates

The cost estimate for the MGN mission made use of two existing Team X studies. One of these studies designed and costed one powered Mars lander, while the other designed and costed three powered Mars landers. A small sub-team of individuals gathered for a brief Team X session in which the bounding cases of the one and three powered landers were altered to generate a quick design and cost for two powered Mars landers. The same cost models and scrutiny were used in this cost estimate.

Tables 5-1 and 5-2 contain costs and workforce by phase for all science activities for the mission (all costs are provided in FY15 dollars).

Phase A for MGN would be nine months long at a cost of approximately \$8M.

Table 5-1. Science Costs by Phase (FY 2015)

	A (\$k)	B (\$k)	C (\$k)	D (\$k)	E (\$k)	F (\$k)	Total (\$k)	ABCD Sum (\$k)
Science	227.7	1,144.8	5,385.8	3,249.7	8,316.7	1,449.2	19,819.0	10,053.0
Science Management	118.0	572.5	1,391.0	1,264.5	1,543.7	436.1	5,325.7	3,346.0
Science Office	118.0	572.5	1,391.0	1,264.5	1,543.7	436.1	5,325.7	3,346.0
Science Implementation	109.7	373.9	3,509.9	1,360.1	2,943.4	755.4	9,052.5	5,353.7
Participating Scientists	36.2	36.2	284.9	287.8	712.2	245.1	1,602.3	645.0
Teams Summary	73.6	337.8	3,225.0	1,072.4	2,231.1	510.3	7,450.2	4,708.7
Science Support	0.0	198.4	485.0	670.0	829.7	257.8	2,440.8	1,353.4
Science Data Archiving	0.0	68.6	167.8	258.1	421.8	137.3	1,053.5	494.5
Instrument Support	0.0	129.8	317.2	411.9	407.9	120.5	1,387.3	858.9
Observatory Program, 2 cycles, 10 people, 150K	0.0	0.0	0.0	0.0	3,000.0	0.0	3,000.0	0.0

Table 5-2. Science Workforce by Phase

	A (W-M)	B (W-M)	C (W-M)	D (W-M)	E (W-M)	F (W-M)	Total (W-M)	Total (W-Y)
Science	5.6	34.3	195.6	111.0	197.0	54.1	597.6	49.8
Science Management	2.5	11.4	29.8	27.1	40.1	12.0	123.0	10.2
Science Office	2.5	11.4	29.8	27.1	40.1	12.0	123.0	10.2
Science Implementation	3.1	13.7	143.2	52.8	119.1	30.4	362.4	30.2
Participating Scientists	1.4	1.4	10.9	11.0	28.5	9.8	62.9	5.2
Teams Summary	1.7	12.4	132.3	41.8	90.6	20.6	299.5	25.0
Science Support	0.0	9.2	22.6	31.0	37.8	11.7	112.3	9.4
Science Data Archiving	0.0	2.9	7.2	11.0	18.0	5.9	44.9	3.7
Instrument Support	0.0	6.3	15.4	20.0	19.8	5.9	67.4	5.6
Science Environmental Characterization	0.0	0.0	0.0	0.0	0.0	0.0	0.0	0.0
Operations Support	0.0	0.0	0.0	0.0	0.0	0.0	0.0	0.0

Table 5-3 shows a detailed funding profile for the MGN mission. Note that there would be no additional cost associated with technology development, due to technology transfer from ESA, enabled by the procurement of the SEIS from ESA's industrial partner. The yearly breakdown in cost is shown in real year dollars with 50% reserves on Phases A–D and 25% reserves on Phase E included in accordance with the NASA ground rules for Decadal Survey studies. Total cost in FY 2015 fixed-year dollars is also shown.

Note that foreign contribution of the SEIS, ATM, and IDA instruments has the potential to reduce the PI-managed mission cost to NASA to \$1094M RY.

Table 5-3. Total Mission Cost Funding Profile

(FY costs¹ in Real Year Dollars, Totals in Real Year and 2015 Dollars)

Item	FY2017	FY2018	FY2019	FY2020	FY2021	FY2022	FY2023	FY2024	FY2025	Total (Real Yr.)	Total (FY2015)
Cost											
Phase A concept study (included below)	0.6	12.3									
Technology development											
	Phase A - D										
Mission PM/SE/MA	0.0	3.2	13.6	18.2	20.0	20.1				75.2	65.0
Pre-launch science	0.0	0.5	2.1	2.8	3.1	3.1				11.6	10.0
Instrument PM/SE	0.0	0.3	1.2	1.6	1.7	1.7				6.4	5.5
Seismometer (ESA)	0.0	1.0	4.1	5.5	6.1	6.1				22.9	19.7
Robotic Arm	0.0	0.5	2.2	2.9	3.2	3.3				12.2	10.5
MET (press., temp., wind, humidity)	0.0	0.6	2.4	3.2	3.5	3.5				13.2	11.4
Cameras	0.0	0.2	0.6	0.9	1.0	1.0				3.6	3.1
Flight Element PM/SE	0.0	2.6	11.3	15.1	16.6	16.7				62.4	53.9
Flight Element (Lander)	0.1	10.4	44.7	59.7	65.7	66.0				246.7	213.1
Flight Element (Entry System)	0.0	2.2	9.3	12.5	13.7	13.8				51.5	44.5
Flight Element (Cruise Stage)	0.0	3.6	15.4	20.6	22.6	22.7				84.9	73.3
MSI&T ²	0.0	1.0	4.5	6.0	27.0	34.6				73.2	62.1
Ground data system dev	0.0	1.1	4.6	6.2	6.8	6.9				25.6	22.1
Navigation & mission design	0.0	0.8	3.5	4.7	5.2	5.2				19.5	16.8
Total dev. w/o reserves	0.4	27.8	119.6	160.0	196.3	204.8				708.8	611.0
Development reserves	0.2	15.0	64.4	86.2	94.8	95.3				355.8	307.4
Total A–D development cost	0.6	42.7	184.0	246.2	291.1	300.1				1064.6	918.4
Launch services			29.5	55.5	61.0	61.3				207.2	178.0
							Phase E				
Phase E science						0.2	4.8	4.9	2.4	12.3	9.8
Other Phase E cost						0.7	16.2	16.6	8.2	41.7	33.0
Phase E reserves						0.3	5.8	6.0	2.9	15.1	11.9
Total Phase E						1.2	26.8	27.5	13.5	69.1	54.7
Education/outreach	0.00	0.08	0.34	0.46	0.51	0.51	2.41	2.48	1.21	8.0	6.6
Other (specify)										0.0	0
Total Cost	\$ 0.6	\$ 42.8	\$ 213.8	\$ 302.1	\$ 352.6	\$ 363.1	\$ 29.2	\$ 30.0	\$ 14.7	\$ 1,349	\$ 1,158
										Total	\$ 1,158

¹ Costs include all costs including any fee

² MSI&T - Mission System Integration and Test and preparation for operations

Appendix A. Acronyms

ACS	attitude control system	IB	isothermal block
ADC	analog-to-digital converter	IDA	instrument deployment arm
ADS	atmospheric dust sensor	IDC	instrument deployment camera
ATM	atmospheric instrument suite	IMU	inertial measurement unit
BOL	beginning of life	IPGP	Institut de Physique du Globe de Paris
CBE	current best estimate	JPL	Jet Propulsion Laboratory
C&DH	command and data handling	MEL	master equipment list
CDR	critical design review	MEPAG	Mars Exploration Program Advisory Group
CG	center of gravity	MER	Mars Exploration Rover
CML	concept maturity level	MEV	maximum expected value
CNES	Centre National d'Études Spatiales (French National Center of Space Research)	MGN	Mars Geophysical Network
CSA	Canadian Space Agency	MLI	multilayer insulation
DHMR	dry heat microbial reduction	MOLA	Mars Orbiter Laser Altimeter
DLR	Deutsches Zentrum für Luft- und Raumfahrt e.V. (German Aerospace Center)	MPF	Mars Pathfinder
DOF	degrees of freedom	MPL	Mars Polar Lander
DOR	Differential One-way Ranging	MT	magnetotelluric method
DSN	Deep Space Network	MOS	mission operations system
DTE	direct to Earth	MRO	Mars Reconnaissance Orbiter
EDL	entry, descent, and landing	MVACS	Mars Volatiles and Climate Surveyor
EM	electromagnetic	NRC	National Research Council
EOL	end of life	PLUTO	Planetary Underground Tool
ETH	Swiss Federal Institute of Technology	PPO	Planetary Protection Officer
FMI	Finnish Meteorological Institute	PRT	platinum resistance thermometer
FY	fiscal year	RCS	reaction control system
GDS	ground data system	SDST	small deep space transponder
GEP	Geophysical and Environmental Package	SEIS	seismometer
GNC	guidance, navigation, and control	SLA	super lightweight ablator
HiRISE	High Resolution Imaging Science Experiment	SP	short period
HP ³	heat flow probe	TC	thermocouple
		TCM	trajectory correction maneuver
		TPS	thermal protection system
		UHF	ultra-high frequency

VBB	very broad band
WEM	warm electronics module
WEB	work breakdown structure

Appendix B. References

- [1] Jet Propulsion Laboratory. (2010), Mars Geophysical Network Mission Concept Trade Study. In review.
- [2] Frey, H. V., J. H. Roark, K. M. Shockey, E. L. Frey, and S. E. H. Sakimoto (2002), Ancient lowlands on Mars, *Geophys. Res. Lett.*, **29**, doi: 10.1029/2001GL013832.
- [3] Stevenson, D. J. (2001), Mars' core and magnetism, *Nature*, **412**, 214–219.
- [4] Breuer D., and Spohn T. (2003), Early plate tectonics versus single-plate tectonics on Mars: Evidence from magnetic field history and crust evolution, *J. Geophys. Res.*, **108**(E7), 8-1, CitelID: 5072, doi: 10.1029/2002JE001999.
- [5] Breuer D., and Spohn T. (2006), Viscosity of the Martian mantle and its initial temperature: Constraints from crust formation history and the evolution of the magnetic field, *Planet. Space Sci.*, **54**(2), 153–169, 10.1016/j.pss.2005.08.008.
- [6] Schumacher S., and Breuer D., 2006, Influence of a variable thermal conductivity on the thermochemical evolution of Mars, *J. Geophys. Res.*, **111**(E2), CitelID: E02006, doi: 10.1029/2005JE002429.
- [7] Dehant, V., H. Lammer, Y. Kulikov, J. M. Grießmeier, D. Breuer, O. Verhoeven, Ö. Karatekin, T. Van Hoolst, O. Korablev and P. Lognonné (2007), Planetary Magnetic Dynamo Effect on Atmospheric Protection of Early Earth and Mars, in *Geology and Habitability of Terrestrial Planets*, eds. K. Fishbaugh, P. Lognonné, F. Raulin, D. Des Marais, O. Korablev, *Space Science Series of ISSI*, vol. **24**, reprinted from *Space Science Reviews*, Springer, Dordrecht, The Netherlands, Space Science Reviews, doi: 10.1007/s11214-007-9163-9, 279-300.
- [8] Dehant, V., W. Folkner, E. Renotte, D. Orban, S. Asmar, G. Balmino, J.-P. Barriot, J. Benoist, R. Biancale, J. Biele, F. Budnik, S. Burger, O. de Viron, B. Häusler, Ö. Karatekin, S. Le Maistre, P. Lognonné, M. Menvielle, M. Mitrovic, M. Pätzold, A. Rivoldini, P. Rosenblatt, G. Schubert, T. Spohn, P. Tortora, T. Van Hoolst, O. Witasse, and M. Yseboodt (2009), Lander Radioscience for obtaining the rotation and orientation of Mars, *Planet. Space Sci.*, **57**, 1050-1067, doi: 10.1016/j.pss.2008.08.009.
- [9] Breuer, D., D. A. Yuen, and T. Spohn (1997), Phase transitions in the Martian mantle: Implications for partially layered convection, *Earth Planet. Sci. Lett.*, **148**(3–4), 457–469, doi: 10.1016/S0012-821X(97)00049-6.
- [10] Spohn, T., M. H. Acuña, D. Breuer, M. Golombek, R. Greeley, A. Halliday, E. Hauber, R. Jaumann, and F. Sohl (2001), Geophysical Constraints on the Evolution of Mars, *Space Sci. Rev.*, **96**(1/4), 231–262.
- [11] Van Thienen, P., K. Benzerara, D. Breuer, C. Gillmann., S. Labrosse, P. Lognonné, and T. Spohn (2007), Water, Life, and Planetary Geodynamical Evolution, in *Treatise of Geophysics*, Elsevier, eds. T. Herring and J. Schubert, **129**(1–3), 167–203, doi: 10.1007/s11214-007-9149-7.
- [12] Spohn, T., F. Sohl., and D. Breuer (1998), Mars, *Astron. Astrophys. Rev.*, **8**(3), 181–235.
- [13] Goins, N. R., and A. R. Lazarewicz (1979), Martian seismicity, *Geophys. Res. Lett.* **6**, 368–370.
- [14] Nakamura, Y., and D. L. Anderson (1979), Martian wind activity detected by a seismometer at Viking lander 2 site, *Geophys. Res. Lett.*, **6**, 499–502.
- [15] Phillips, R. J. (1991), Expected rate of marsquakes, in *Scientific Rationale and Requirements for a Global Seismic Network on Mars*, *LPI Tech. Rept. 91-02*, Lunar and Planetary Inst., Houston. pp. 35-38.
- [16] Golombek, M. P., W. B. Banerdt, K. L. Tanaka, and D. M. Tralli (1992), A prediction of Mars seismicity from surface faulting, *Science*, **258**, 979–981.

- [17] Knapmeyer, M., J. Oberst, E. Hauber, M. Wählisch, C. Deuchler, and R. Wagner (2006), Implications of the martian surface fault distribution and lithospheric cooling for seismicity: a working model, *J. Geophys. Res.* **111**, E11006.
- [18] Davis, P. M. (1993), Meteoroid impacts as seismic sources on Mars, *Icarus*, **105**, 469–478.
- [19] Lognonné, P., and C. Johnson (2007), Planetary Seismology, in *Treatises in Geophysics*, G. Schubert, ed., sec. 10.04, Elsevier.
- [20] Lognonné, P., J. Gagnepain-Beyneix, W. B. Banerdt, S. Cacho, J.-F. Karczewski, and M. Morand (1996), An ultra broad band seismometer on InterMarsnet, *Planet. Space Sci.* **44**, 1237–1249.
- [21] Mocquet, A. (1999), A search for the minimum number of stations needed for seismic networking on Mars, *Planet. Space Sci.*, **47**, 397–409.
- [22] Gudkova, T. V., and V. N. Zharkov (2004), Mars: interior structure and excitation of free oscillations, *Phys. Earth Planet. Int.*, **142**, 1–22.
- [23] Sohl, F., and T. Spohn (1997), The interior structure of Mars: Implications from SNC meteoroids, *J. Geophys. Res.*, **102**, 1613–1636.
- [24] Shapiro, N. M., and M. Campillo (2004), Emergence of broadband Rayleigh waves from correlations of the ambient seismic noise, *Geophys. Res. Lett.*, **31**, doi: 10.1029/2004GL019491.
- [25] Cazenave, A., and G. Balmino (1981), Meteorological effects on the seasonal variations of the rotation of Mars, *Geophys. Res. Lett.*, **8**, 245–248.
- [26] Chao, B. F., and D. P. Rubincam (1990), Variations of Mars gravitational field and rotation due to seasonal CO₂ exchange, *J. Geophys. Res.*, **95**, 14755–14760.
- [27] Folkner, W. M., C. F. Yoder, D. N. Yuan, E. M. Standish, and R. A. Preston (1997), Interior Structure and Seasonal Mass Redistribution of Mars from Radio Tracking of Mars Pathfinder, *Science*, **278**(5344), 1749–1751.
- [28] Yoder, C. F., and E. M. Standish (1997), Martian moment of inertia from Viking lander range data, *J. Geophys. Res.*, **102** (E2), 4065–4080.
- [29] Defraigne, P., O. de Viron, V. Dehant, T. Van Hoolst, and F. Hourdin (2000), Mars rotation variations induced by atmospheric CO₂ and winds, *J. Geophys. Res.*, **105**, E10, 24563–24570.
- [30] Dehant V., O. de Viron, Ö. Karatekin, and T. Van Hoolst (2006), Excitation of Mars polar motion, *Astron. Astrophys.*, **446**(1), doi: 10.1051/0004-6361:20053825, 345–355.
- [31] Van den Acker, E., T. Van Hoolst, O. de Viron, P. Defraigne, V. Dehant, F. Forget, and F. Hourdin (2002), Influence of the winds and of the CO₂ mass exchange between the atmosphere and the polar ice caps on Mars' orientation parameters, *J. Geophys. Res.*, 10.1029/2000JE001539.
- [32] Sanchez, B., R. Haberle, and J. Schaeffer (2004), Atmospheric rotational effects on Mars based on the NASA Ames general circulation model: Angular momentum approach, *J. Geophys. Res.*, **109**(E8), CiteID: E08005, doi: 10.1029/2004JE002254.
- [33] Karatekin, Ö., J. Duron, P. Rosenblatt, V. Dehant, T. Van Hoolst, and J.-P. Barriot (2005), Martian Time-Variable Gravity and its Determination; Simulated Geodesy Experiments, *J. Geophys. Res.*, **110**(E6), CiteID: E06001, doi: 10.1029/2004JE002378.
- [34] Karatekin, Ö., T. Van Hoolst, J. Tastet, O. de Viron, and V. Dehant (2006), The effects of seasonal mass redistribution and interior structure on Length-of-Day variations of Mars, *Adv. Space Res.*, **38**(4), 561-828, doi: JASR-D-04-01301R1.
- [35] Karatekin, Ö., V. Dehant, and T. Van Hoolst (2006), Martian global-scale CO₂ exchange from time-variable gravity measurements, *J. Geophys. Res.*, **111**, CiteID: E06003, doi: 10.1029/2005JE002591.

- [36] Zuber, M., F. Lemoine, D. Smith, A. Konopliv, S. Smrekar, and S. Asmar (2007), The Mars Reconnaissance Orbiter Radio Science Gravity Investigation, *J. Geophys. Res.*, **112**, Issue E5, CiteID E05S07, doi: 10.1029/2006JE002833.
- [37] Schulze-Makuch, D., and L. N. Irwin (2008), *Life in the Universe – Expectations and Constraints*, 2nd edition, Springer.
- [38] Sonett, C. (1982), Electromagnetic Induction in the Moon, *Rev. Geophys.*, **20**(3), 411-455.
- [39] Khurana, K. K., M. G. Kivelson, D. J. Stevenson, G. Schubert, C. T. Russell, R. J. Walker, and C. Polansky (1998), Induced magnetic fields as evidence for subsurface oceans in Europa and Callisto, *Nature*, **395**, 777–780.
- [40] Hood, L., D. Mitchell, R. Lin, M. Acuña, and A. Binder (1999), Initial Measurements of the Lunar Induced Magnetic Dipole Moment Using Lunar Prospector Magnetometer Data, *Geophys. Res. Lett.*, **26**(15), 2327–2330.
- [41] Wait, J. R., (1970), *Electromagnetic Waves in Stratified Media*, Pergamon, New York.
- [42] Grimm R. E. (2002), Low-frequency electromagnetic exploration for groundwater on Mars, *J. Geophys. Res.*, **107**(E2), 5006, doi: 10.1029/ 2001JE001504.
- [43] Gough, D. I., and M. R. Ingham (1983), Interpretation methods for magnetometer arrays, *Rev. Geophys.*, **21**, 805–827.
- [44] Espley J. R., G. T. Delory, and P. A. Cloutier (2006), Initial observations of low-frequency magnetic fluctuations in the Martian ionosphere, *J. Geophys. Res.*, **111**, E06S22, doi:10.1029/2005JE002587.
- [45] Rafkin, S., et al. (2009), *The Value of Landed Meteorological Investigations on Mars: The Next Advance for Climate Science*, White Paper submitted Sept. 15, 2009 to the National Research Council's 2009 Planetary Decadal Survey.